DARK ENERGY FROM SINGLE SCALAR FIELD MODELS

CHAKKRIT KAEONIKHOM

A Thesis Submitted to the Graduate School of Naresuan University

in Partial Fulfillment of the Requirements

for the Master of Science Degree in Physics

September 2011

This thesis entitled "Dark Energy from Single Scalar Field Models" submitted by Chakkrit Kaeonikhom in partial fulfillment of the requirements for the Master of Science in Physics is hereby approved.

.... Chair
(Teeraparb Chantavat, D.Phil.)

.... Committee
(Burin Gumjudpai, Ph.D.)

.... Committee
(Nattapong Yongram, Ph.D.)

.... Committee
(Assistant Professor Piyabut Burikham, Ph.D.)

Approved

....
(Assistant Professor Kanungnit Pupatwibul, Ph.D.)
Dean of the Graduate School
September 2011

ACKNOWLEDGEMENTS

I would like to thank my advisor, Dr. Burin Gumjudpai for giving me the motivation of this thesis, useful discussion and for everything. I would like to thank Dr. Nattapong Yongram, Dr. Teeraparb Chantavat and Mr. Rachan Rangdee for spending time to discussion. Thank Emmanuel N. Saridakis, my collaborator for co-working in part of this thesis. I would like to thank Dr. Chanun Sricheewin for some discussions. I also thank Ms. Sasithorn Thanad for giving morale to me. Finally, thank to the great kindness of my mother who gave me the great morale and everything. I am supported by a Graduate Assistantship funded by the Thailand Center of Excellence in Physics (ThEP).

Chakkrit Kaeonikhom

LIST OF CONTENTS

Chapter **Page**

I INTRODUCTION 1
Background and motivation 1
Objectives 2
Frameworks 2

II STANDARD COSMOLOGY 3
The cosmological principle and Weyl's postulate 3
Hubble's law 4
A brief review of Friedmann-Lemaître-Robertson-Walker universe . 5
Why dark energy? 11

III DARK ENERGY MODELS 20
Cosmological constant 20
Scalar field models of dark energy 23

IV PHANTOM POWER-LAW COSMOLOGY 29
Phantom cosmology with power-law expansion 29
Observational constraints 32
Results and discussions 33

V CONCLUSIONS 38

REFERENCES 40

APPENDICES 48

BIOGRAPHY 79

LIST OF TABLES

Table **Page**

1 Non-zero coefficients of Cristoffel symbols for FLRW matric.................... 7

2 The maximum likelihood values in 1σ confidence level for the present time t_0, the Hubble parameter H_0, the present baryon density parameter Ω_{b0} and the present cold dark matter density parameter Ω_{CDM0}, for WMAP7 as well as for the combined fitting WMAP7+BAO+ H_0. The values are taken form [33]............................ 34

3 Derived maximum likelihood values in 1σ confidence level for the power law exponent β, the present matter energy density values ρ_{m0}, the present critical energy density ρ_{c0} and the big rip time t_s, for WMAP7 as well as for the combined fitting WMAP7+ BAO+ H_0 35

4 The table is shown the true values, which using $w_{DE} = -1.10$ [33] from WMAP7+BAO+ H_0. The changed value from Table 3 are power-law exponent and the big rip time, while other parameters remain the same.. 48

5 Relation between the value of dark energy equation-of-state parameter w_{DE} and the value of big rip time t_s.................................... 50

LIST OF FIGURES

Figure **Page**

1 Plotting of the age of the universe and density parameter of matter shows that flat universe with dark energy (solid line) is consistent with WMAP 7-year bound. We see that the matter contributed in the universe is indeed about 28%, and dark energy is 72%. 14

2 Plotting of the scale factor $a(t)$ versus $H_0(t-t_0)$ shows that the universe with dark energy (the solid line) gives accelerating expansion while dust model without dark energy (the dashed line) cannot give accelerating universe. 15

3 Plotting of the luminosity distance versus redshift of SN Ia for flat cosmological model. Most data from SN Ia correspond to $\Omega_{\mathrm{DE}} \simeq 0.7$ (the solid line) 18

4 Plotting of the luminosity distance versus redshift for flat FLRW model. The black points are taken form the "Gold" dataset by Riess *et al.* [50], and the red points are taken from HST data measured in 2003. This figure is taken from Ref. [16] 19

5 The phantom potential as function of t, obtained from observational data fitting of WMAP7 and WMAP7+BAO+ H_0 35

6 The phantom potential as function of ϕ, obtained from observational data fitting of WMAP7 and WMAP7+BAO+ H_0 37

7 The phantom potential of the true value for WMAP7+BAO+ H_0 dataset WMAP7 dataset alone 49

8 Plotting of big rip time t_s versus equation-of-state parameter of dark energy w_{DE} 50

Title	DARK ENERGY FROM SINGLE SCALAR FIELD MODELS
Author	Chakkrit Kaeonikhom
Advisor	Burin Gumjudpai, Ph.D.
Co-Advisor	Nattapong Yongram, Ph.D.
Academic Paper	Thesis M.S. in Physics, Naresuan University, 2011
Keywords	Dark Energy, Scalar Field, Phantom Power-law Cosmology, WMAP 7-years data

ABSTRACT

It has been known that dust dominated cosmological model has many problems to explain accelerating universe which was found in 1998 by Riess *et al.* and Perlmutter *et al.* [49][48]. Many models of universe are proposed under hypothesis that dark energy causes acceleration of the universe. We study dark energy focusing to single scalar field models. We briefly review dark energy models namely quintessence, phantom and tachyon models. In particular, we investigate phantom cosmology in which the scale factor is of power-law function. We use cosmological observations from Cosmic Microwave Background (CMB), Baryon Acoustic Oscillations (BAO) and observational Hubble data, in order to impose complete constraints on the model parameters. We find that the power-law exponent is $\beta = 6.51^{+0.24}_{-0.25}$, while the big rip is realized at $t_{\mathrm{s}} = 104.5^{+1.9}_{-2.0}$ Gyr, in 1σ confidence level. Providing late-time asymptotic expressions and power-law nature of $a(t)$, we find that the dark-energy equation-of-state parameter at the big rip remains finite and equal to $w_{\mathrm{DE}} = -1.153$, with the dark-energy density and pressure diverging. Finally, we reconstruct the phantom potential.

CHAPTER I

INTRODUCTION

1.1 Background and motivation

Mathematical implication by Friedmann and others within Einstein's general relativity tells us that the universe is expanding. A strong evidence corresponding to the predictions is that all the observed objects in deep space are redshifted. This means that these objects are receding from the Earth. This phenomenon obeys a law known as Hubble's law, which Hubble was found empirically in 1929 [24]. However, the law was first derived from general relativity by Georges Lemaître in 1927 [36].

The simplest cosmological model assumes that the universe is filled with both matter (slowly moving particles i.e., galaxies, nebulae and so on) and radiation. Nowadays, it was found that radiation density is much less than matter density therefore the universe today is assumed to be matter dominated. If matter can be treated as a pressureless fluid, then the universe will expand forever (if the spatial geometry is Euclidean or hyperbolic) or eventually recollapse (if the spatial geometry is of a 3-sphere) [53].

In 1998, published observations of type Ia supernovae by the High-z Supernova Search Team [49], followed in 1999 by the Supernova Cosmology Project [48], suggested that the expansion of the universe is accelerating. The observational evidences indicate that the universe can not be modeled in such a simple way. A hypothesis corresponding to the observations is that the universe may consist of some form of *dark energy* with negative-pressure. The existence of dark energy is needed to reconcile the measured geometry of space by measurements of the cosmic microwave background (CMB) anisotropies, most recently by the WMAP satellite. The CMB indicates that the universe is very close to flatness [33, 35]. The WMAP seven-year analysis gives an estimate of 72.7% dark energy, 22.7% dark matter and 4.6% ordinary matter. The first model of dark energy is "cosmological constant" that give equation-of-state parameter $w = -1$.

This model has an unsolved problem, namely its observed energy scale from astrophysics is much different from vacuum energy in particle physics [55]. This leads to scalar field model of dark energy which gives time-dependent equation of state.

1.2 Objectives

We study single scalar field models of dark energy, especially phantom dark energy, a dark energy model with w less than minus one. We apply power-law expansion of the universe to phantom dark energy. Our objectives are to obtain phantom potential, scalar field solution, and the big rip time. These result can be used to predict equation of state of phantom energy at late time.

1.3 Frameworks

We review basic cosmology in the Chapter 2, and roughly review single scalar field models of dark energy in the Chapter 3. Chapter 4 is dedicated to a model of dark energy called "phantom energy" [9]. In this work, we aim to impose observational constraints on phantom power-law cosmology. That is on the scenario of a phantom scalar field with the matter fluid in which the scale factor is power law in time. In particular, we use cosmological observations from Cosmic Microwave Background (CMB), Baryon Acoustic Oscillations (BAO) and Hubble Space Telescope data (HST, H_0), in order to impose complete constraints on the model parameters, e.g. the power-law exponent, w and on the big rip time. In this chapter, we use the observational data to impose constraints on the model parameters, reconstructing the phantom potential and solving for phantom scalar field solution. Finally we determine equation-of-state parameter of phantom dark energy at late time. The last Chapter is the conclusions.

CHAPTER II

STANDARD COSMOLOGY

2.1 The cosmological principle and Weyl's postulate

Modern cosmology is based on *cosmological principle.* It is believed that the universe on large scales possesses two important properties, **homogeneity** and **isotropy** at a *particular time.* Homogeneity means the universe looks the same everywhere. There is no special location in the universe. Isotropy means the universe looks the same in all directions. Note that homogeneity does not imply isotropy and vice versa, e.g. a uniform electric field is a homogeneous field, at all points the field is the same, but it is not isotropic at one point because directions of the field lines can be distinguished. Alternatively, if we are in the center of a ball, we can see that all directions are the same, it is isotropic but not necessarily homogeneous. However, if isotropy is required at every point, the universe is automatically enforced to be homogeneous. Mathematical language of homogeneity and isotropy are translational invariant and rotational invariant respectively.

The cosmological principle needs to be defined at particular time. In special relativity, the concept becomes well-defined if one chooses a particular inertial frame but in general relativity the concept of global inertial frames is not defined. A postulate known as Weyl's postulate is (d'Inverno's book [25])

> *The particles of the substratum lie in spacetime on a congruence of timelike geodesics diverging from a point in the finite or infinite past,*

which requires that some observersare moving in a local Lorentz frame whose worldlines are bundles or congruences[1]. These trajectories are non-intersecting. Only one trajectory passes through a point in space. The number of local inertial observers can be infinite and continuous at all points in space. The observers which obey these conditions

[1]The observers can be at anywhere or at any points in spacetime.

are called *fundamental observer*. The Weyl's postulate allows us to introduce a series of non-intersecting spacelike hypersurface which all observers lie on. The hypersurface is surface of simultaneity of the local Lorentz frame of any fundamental observers [23, 26]. Thus, the 4-velocity of any observers is orthogonal to the hypersurfaces. This series of hypersurfaces is labeled by proper time of any stationary observers. This defines a universal time so that a particular time means a given spacelike hypersurface on the series of hypersurface. The time $t =$ constant of each hypersurface is the *cosmic time*.

2.2 Hubble's law

Hubble discovered that most galaxies are receding from the Earth. Hubble realized a linear relation between recessional velocity and distance in term of mathematical expression:

$$v = H_0 r, \tag{2.1}$$

where r is the physical distance. This is known as **Hubble's law** and the constant H_0 is known as the Hubble's constant at present time. These galaxies' velocities are measured via redshift, which is Doppler's effect of light. The Hubble's constant is usually parameterized as

$$H_0 = 100h \ \ \mathrm{km\,s^{-1}Mpc^{-1}}. \tag{2.2}$$

The result from WMAP 7-year data combined with Baryon Acoustic Oscillations (BAO) and Hubble constant (H_0) measurement gives [33]

$$h = 0.704^{+0.013}_{-0.014}, \tag{2.3}$$

with one-sigma error. The radial motion of a galaxy required by cosmological principle implies that, at a particular cosmic time t, the distance $r^i(t)$ of the ith galaxy from us is given by

$$r^i(t) = a(t)x^i(t_0) \tag{2.4}$$

where homogeneity property is applied so that a, the *scale factor*, is a function of cosmic time alone. The Eq. (2.4) implies that the expanding universe is indeed the expansion of coordinate grid with time. Therefore the galaxies remain at fixed location in the $x^i(t_0)$ coordinate system, the *comoving coordinate*, which is fixed by definition in a cosmic time t_0. The radial (expanding) velocity of the ith galaxy is given by

$$\dot{r}^i(t) = \dot{a}(t)x^i(t_0) = \frac{\dot{a}(t)}{a(t)}r^i(t). \tag{2.5}$$

The Hubble parameter $H(t)$ hence, defined as

$$H(t) \equiv \frac{\dot{a}(t)}{a(t)}, \tag{2.6}$$

and the Hubble's law can be written as $\dot{r}^i(t) = H(t)r^i(t)$. Note that the value as measured today is denoted by a subscript "0" as H_0.

2.3 A brief review of Friedmann-Lemaître-Robertson-Walker universe

A solution of Einstein's field equations in general relativity that describes our universe is the Friedmann-Lemaître-Robertson-Walker metric (FLRW metric). In deriving of the FLRW metric, a metric satisfying the Weyl's postulate must be considered. The spatial component of the metric can be time dependent and it is therefore written in the form

$$\mathrm{d}s^2 = c^2\mathrm{d}t^2 - a^2(t)\mathrm{d}\Sigma^2 \tag{2.7}$$

where $\mathrm{d}\Sigma^2 = \gamma_{ij}\mathrm{d}x^i\mathrm{d}x^j$ is the spacelike hypersurface, and γ_{ij} is only function of (x^1, x^2, x^3). If $x(\tau)$ is the observer's worldline, where τ labels proper time of the observer along the worldline, according to Weyl's postulate, the proper time for any observers on a hypersurface is indeed the cosmic time coordinate. The factor $a(t)$ is dimensionless scale factor, a function of cosmic time. The spacelike hypersurface metric $\mathrm{d}\Sigma$ satisfying these above conditions is $\mathrm{d}\Sigma^2 = \mathrm{d}r^2/(1-kr^2) + r^2(\mathrm{d}\theta^2 + \sin^2\theta\,\mathrm{d}\phi^2)$ as in standard text books [23, 25, 26]. The full FLRW metric in the coordinates $x^\mu = (t, r, \theta, \phi)$ is then taken the form

$$\mathrm{d}s^2 = c^2\mathrm{d}t^2 - a^2(t)\left[\frac{\mathrm{d}r^2}{1-kr^2} + r^2(\mathrm{d}\theta^2 + \sin^2\theta\,\mathrm{d}\phi^2)\right], \tag{2.8}$$

where the curvature k is constant and is independent of coordinates. The hypersurface $\mathrm{d}\Sigma$ can have flat geometry, spherical geometry, or hyperbolic geometry when the k value is rescaled to $\{0, 1, -1\}$ respectively. The coordinates x^μ in FLRW metric is indeed the comoving coordinates mentioned earlier. The metric (2.8) may be parametrized with χ in form of

$$\mathrm{d}s^2 = c^2\mathrm{d}t^2 - a^2(t)\left[\mathrm{d}\chi^2 + f_k^2(\chi)(\mathrm{d}\theta^2 + \sin^2\theta\,\mathrm{d}\phi^2)\right], \tag{2.9}$$

where

$$f_k(\chi) = \begin{cases} \sin\chi, & k = +1 \\ \chi, & k = 0 \\ \sinh\chi, & k = -1. \end{cases}$$

Note that the function $f_k(\chi)$ can be written in unified form for $k \neq 0$ as

$$f_k(\chi) = \frac{1}{\sqrt{-k}}\sinh\left(\sqrt{-k}\chi\right), \tag{2.10}$$

which might be more convenient to use later.

2.3.1 Friedmann equations

Cosmological equations can be derived by imposing the FLRW metric to the Einstein's field equations with source term, the energy-momentum tensor $T_{\mu\nu}$, which is taken as a perfect fluid. The Einstein's field equation is

$$G_{\mu\nu} \equiv R_{\mu\nu} - \frac{1}{2}g_{\mu\nu}R = \frac{8\pi G}{c^4}T_{\mu\nu}, \tag{2.11}$$

where $G_{\mu\nu}$ is Einstein tensor defined in the terms of metric $g_{\mu\nu}$, Ricci tensor $R_{\mu\nu}$ and Ricci scalar R. $T_{\mu\nu}$ is energy-momentum tensor. However, Einstein's field equations can be expressed in alternative form

$$R_{\mu\nu} = \frac{8\pi G}{c^4}\left(T_{\mu\nu} - \frac{1}{2}Tg_{\mu\nu}\right), \tag{2.12}$$

where $T \equiv T^\mu_\mu$. The Cristoffel symbols is given in terms of the FLRW metric,

$$\Gamma^\sigma_{\mu\nu} = \frac{1}{2}g^{\sigma\rho}\left(\partial_\nu g_{\rho\mu} + \partial_\mu g_{\rho\nu} - \partial_\rho g_{\mu\nu}\right).$$

Using the metric components of FLRW metric, the non-zero coefficients of Cristoffel symbols are straightforward calculated as in Table 1 where the dots denote differen-

$\Gamma^1{}_{11} = kr/(1-kr^2)$	$\Gamma^1{}_{01} = \Gamma^2{}_{02} = \Gamma^3{}_{03} = \dot{a}/a$
$\Gamma^3{}_{13} = \Gamma^2{}_{12} = 1/r$	$\Gamma^0{}_{33} = a\dot{a}r^2\sin^2\theta/c^2$
$\Gamma^1{}_{22} = -r(1-kr^2)$	$\Gamma^2{}_{33} = -\sin\theta\cos\theta$
$\Gamma^0{}_{11} = a\dot{a}/c^2(1-kr^2)$	$\Gamma^1{}_{33} = -r(1-kr^2)\sin^2\theta$
$\Gamma^3{}_{23} = \cos\theta/\sin\theta$	$\Gamma^0{}_{22} = a\dot{a}r^2/c^2$

Table 1. Non-zero coefficients of Cristoffel symbols for FLRW matric

tiation with respect to the cosmic time t. Substituting these non-zero coefficients of Cristoffel symbols into the expression of the Ricci tensor,

$$R_{\mu\nu} = R^\rho{}_{\mu\rho\nu} = \partial_\sigma\Gamma^\sigma{}_{\mu\nu} - \partial_\nu\Gamma^\sigma{}_{\mu\sigma} + \Gamma^\rho{}_{\mu\nu}\Gamma^\sigma{}_{\rho\sigma} - \Gamma^\rho{}_{\mu\sigma}\Gamma^\sigma{}_{\rho\nu}.$$

Thus, according to Table 1, the components of the Ricci tensor are given by

$$\begin{aligned}
R_{00} &= -\frac{3\ddot{a}}{a}, \\
R_{11} &= \frac{a\ddot{a} + 2\dot{a}^2 + kc^2}{c^2(1-kr^2)}, \\
R_{22} &= (a\ddot{a} + 2\dot{a}^2 + 2kc^2)r^2/c^2, \\
R_{33} &= (a\ddot{a} + 2\dot{a}^2 + 2kc^2)r^2\sin^2\theta/c^2.
\end{aligned}$$

The off-diagonal components of the Ricci tensor are zero. Next step is to consider the energy-momentum tensor in Einstein's field equations. According to the Weyl's postulate, only one observer's geodesic can pass through each point of spacetime, and consequently the observer at any point possesses a unique velocity. Therefore any observer or any particle can be considered as perfect fluid. Thus, the energy-momentum tensor $T_{\mu\nu}$ in the field equations is assumed to be of a 'cosmic' perfect fluid, which is described by

$$T^{\mu\nu} = \left(\rho + \frac{p}{c^2}\right)u^\mu u^\nu - pg^{\mu\nu}, \tag{2.13}$$

where u^μ is 4-velocity. ρ and p are, respectively, mass density and pressure, which are only functions of cosmic time because the universe is assumed to be homogeneous and isotropic. Since all observers possess each local Lorentz frame, their 4-velocities are simply

$$u^\mu = (1,0,0,0). \tag{2.14}$$

The covariant component of the 4-velocity is $u_\mu = g_{\mu\nu}u^\nu$, $u_0 = g_{0\nu}u^\nu = (c^2, 0, 0, 0)$ and hence $u_\mu = c^2\delta^0_\mu$ therefore the energy-momentum tensor in covariant component is in the form

$$T_{\mu\nu} = g_{\mu\rho}g_{\nu\sigma}T^{\rho\sigma} = \left(\rho + \frac{p}{c^2}\right) g_{\mu\rho}g_{\nu\sigma}u^\rho u^\sigma - pg_{\mu\nu} = \left(\rho c^2 + p\right) c^2\delta^0_\mu\delta^0_\nu - pg_{\mu\nu}. \quad (2.15)$$

Contraction of energy-momentum tensor gives

$$T = T^\mu{}_\mu = \left(\rho + \frac{p}{c^2}\right) u_\mu u^\mu - p\delta^\mu_\mu = \rho c^2 - 3p, \quad (2.16)$$

where $u^\mu u_\mu = c^2$. Connecting the curvature terms to the matter terms following Eq. (2.12) yields two independent equations which are called *Friedmann equations*, which taking the form

$$\frac{\ddot{a}}{a} = -\frac{4\pi G}{3}\left(\rho + \frac{3p}{c^2}\right), \quad (2.17)$$

$$H^2 = \frac{8\pi G}{3}\rho - \frac{kc^2}{a^2}, \quad (2.18)$$

where $H = \dot{a}/a$. Note that the first equation is usually known as called *acceleration equation*.

2.3.2 Fluid equation

The fluid equation in FLRW universe can be derived by taking divergence to the energy-momentum tensor. The conservation of energy-momentum tensor requires

$$\nabla_\mu T^{\mu\nu} = 0. \quad (2.19)$$

Considering divergence of the energy-momentum tensor for perfect fluid, Eq. (2.13), which is given by

$$\begin{aligned} \nabla_\mu T^{\mu\nu} &= \nabla_\mu \left[\left(\rho + \frac{p}{c^2}\right) u^\mu u^\nu - pg^{\mu\nu}\right] \\ &= u^\nu \nabla_\mu \left[\left(\rho + \frac{p}{c^2}\right) u^\mu\right] + \left(\rho + \frac{p}{c^2}\right) u^\mu \nabla_\mu u^\nu - g^{\mu\nu}\nabla_\mu p. \end{aligned}$$

Since each worldline in cosmological fluid particle is geodesic path which requires that $u^\mu\nabla_\mu u^\nu = 0$, hence the second term on right-hand-side in second line of the equation above vanishes. Thus, conservation of the energy-momentum tensor gives

$$\left[u^\mu u^\nu \nabla_\mu \left(\rho + \frac{p}{c^2}\right) + u^\nu \left(\rho + \frac{p}{c^2}\right) \nabla_\mu u^\mu\right] - g^{\mu\nu}\nabla_\mu p = 0.$$

Expanding the covariant derivative as $\nabla_\mu A^\nu = \partial_\mu A^\nu + \Gamma^\nu{}_{\mu\lambda} A^\lambda$, and using the fact that covariant derivative of any scalar field ϕ is indeed equal to partial derivative such as $\nabla_\mu \phi = \partial_\mu \phi$, thus the equation above becomes

$$u^\mu u^\nu \partial_\mu \left(\rho + \frac{p}{c^2}\right) + u^\nu \left(\rho + \frac{p}{c^2}\right) \left[\partial_\mu u^\mu + \Gamma^\mu{}_{\mu\lambda} u^\lambda\right] - g^{\mu\nu}\partial_\mu p = 0.$$

Since the assumptions of FLRW universe are homogeneity and isotropy therefore the mass density and pressure are only function of cosmic time. We therefore have

$$u^0 u^0 \partial_0 \rho + \frac{u^0 u^0}{c^2}\partial_0 p + u^0 \left(\Gamma^1{}_{10} + \Gamma^2{}_{20} + \Gamma^3{}_{30}\right)\left(\rho + \frac{p}{c^2}\right) - g^{00}\partial_0 p = 0.$$

The second term and the last terms on the left hand side cancel out. Using expression of the coefficients of the Cristoffel symbols in Table 1, we get

$$\dot{\rho} + 3H\left(\rho + \frac{p}{c^2}\right) = 0. \tag{2.20}$$

This is called cosmological fluid equation.

2.3.3 Cosmological redshift

In astrophysics, the redshift z of moving light source is defined as

$$z = \frac{\lambda_{\text{obs}} - \lambda_{\text{em}}}{\lambda_{\text{em}}} \quad \text{or} \quad z = \frac{\nu_{\text{em}} - \nu_{\text{obs}}}{\nu_{\text{obs}}}, \tag{2.21}$$

where λ and ν are wavelengths and frequency of light. The subscript "em" and "obs" denote emitted and observed photon respectively. The light ray follows null geodesic, $\mathrm{d}s = 0$ and $\mathrm{d}\theta = \mathrm{d}\phi = 0$ along the photon path. Therefore, using the Eq. (2.9) we have

$$\int_{t_{\text{em}}}^{t_{\text{obs}}} \frac{c\,\mathrm{d}t}{a(t)} = \int_0^{\chi_{\text{em}}} \mathrm{d}\chi = \chi_{\text{em}}, \tag{2.22}$$

where χ is coordinate relating to r as $r = \chi$ for $k = 0$, $r = \sin\chi$ for $k = 1$ and $r = \sinh\chi$ for $k = -1$. If next light pulse was sent from the galaxy at time $t_{\text{em}} + \delta t_{\text{em}}$, which is received at time $t_{\text{obs}} + \delta t_{\text{obs}}$, then

$$\int_{t_{\text{em}}+\delta t_{\text{em}}}^{t_{\text{obs}}+\delta t_{\text{obs}}} \frac{c\,\mathrm{d}t}{a(t)} = \int_0^{\chi_{\text{em}}} \mathrm{d}\chi = \int_{t_{\text{em}}}^{t_{\text{obs}}} \frac{c\,\mathrm{d}t}{a(t)}.$$

Assuming $\delta t_{\rm em}$ and $\delta t_{\rm obs}$ are small therefore $a(t)$ can be taken as constant in both integrals, therefore

$$\frac{\delta t_{\rm obs}}{a(t_{\rm obs})} = \frac{\delta t_{\rm em}}{a(t_{\rm em})}.$$

Since the frequency is inversely proportional to the time interval, form Eq. (2.21), we find

$$1+z = \frac{\nu_{\rm em}}{\nu_{\rm obs}} = \frac{a(t_0)}{a(t)} \tag{2.23}$$

where $a(t_{\rm obs})$ and $a(t_{\rm em})$ are renamed to, respectively, $a(t_0)$ and $a(t)$ for simplicity.

2.3.4 Cosmological parameters

In simple cosmological model, the universe is assumed to be filled with matter and radiation. The total density is simply the sum of the individual contributions of cosmological components:

$$\rho(t) = \rho_{\rm m}(t) + \rho_{\rm r}(t) \tag{2.24}$$

where the subscripts denote mass densities of matter and radiation respectively. Since these cosmological components can be treated as a perfect fluid with an equation of state of the form

$$p = w\rho c^2,$$

where the equation-of-state parameter w is a constant. Hence the Eq. (2.18) with $k = 0$ and Eq. (2.20) give

$$\rho \propto a^{-3(1+w)}, \tag{2.25}$$

$$a \propto t^{\frac{2}{3(1+w)}}, \tag{2.26}$$

where t_0 is constant. Note that the above solutions are valid for $w \neq -1$. In particular $w = 0$ for slowly moving particles or pressureless *dust*. For radiation or, in the sense of particle, photon, an ideal model of photon gas, the pressure of photons is given by $p_{\rm r} = \rho_{\rm r} c^2/3$. Therefore the equation-of-state parameter for radiation is given by $w = 1/3$.

A useful parameter in cosmology is the density parameter, $\Omega(t)$, defined as

$$\Omega(t) \equiv \frac{\rho(t)}{\rho_{\rm c}(t)}, \tag{2.27}$$

where the critical density is given by

$$\rho_{\rm c}(t) \equiv \frac{3H^2(t)}{8\pi G}. \tag{2.28}$$

We can write the Friedmann equation (2.18) in the form

$$\Omega(t) - 1 = \frac{kc^2}{H^2(t)a^2(t)}. \tag{2.29}$$

If one define the curvature density parameter

$$\Omega_k(t) \equiv -\frac{kc^2}{H^2(t)a^2(t)}, \tag{2.30}$$

hence the Friedmann equation becomes

$$\Omega(t) \equiv \Omega_{\rm m}(t) + \Omega_{\rm r}(t) = 1 - \Omega_k(t). \tag{2.31}$$

In summary density contribution determines the spatial geometry of our universe, i.e.

$$\begin{array}{llllllll}
\Omega < 1 & \text{or} & \rho < \rho_{\rm c} & \Leftrightarrow & k = -1 & \Leftrightarrow & \text{open universe} \\
\Omega = 1 & \text{or} & \rho = \rho_{\rm c} & \Leftrightarrow & k = 0 & \Leftrightarrow & \text{flat universe} \\
\Omega > 1 & \text{or} & \rho > \rho_{\rm c} & \Leftrightarrow & k = +1 & \Leftrightarrow & \text{closed universe.}
\end{array}$$

Note that, the total density parameter Ω can be included other cosmological components for more advanced cosmological models.

2.4 Why dark energy?

As we mention in the Chapter 1, the simplest dust model can not describe accelerating universe problem. However this problem can be solved by including a term of "dark energy" in cosmological model. In this section, we discuss for details of some observational evidence for dark energy, and why there should be dark energy needs in the universe.

2.4.1 Problems of dust model

In the present time, radiation density in the universe is much less than matter density. Thus the universe today might be filled with matter (or dust). If it is so, the universe model would not be consistent with observation. Consider acceleration equation (2.17) for dust model, which state that

$$\frac{\ddot{a}}{a} = -\frac{4\pi G}{3}\rho(1+3w). \tag{2.32}$$

Accelerating universe needs $\ddot{a} > 0$, thus we need $1 + 3w < 0$. We can immediately see that if we use $\rho = \rho_{\rm m}$ ($w_{\rm m} = 0$), it can not give accelerating universe. Therefore we need a term of some sort of energy which has $w < -1/3$ in the Friedmann equation. This energy is so called dark energy.

Another problem of dust model is the age of the universe. In flat FRW universe, the dust model gives the solution (2.26) which is

$$a = \left(\frac{t}{t_0}\right)^{2/3}, \tag{2.33}$$

where we set $a_0 = 1$. Thus we have

$$H = \frac{\dot{a}}{a} = \frac{2}{3t}. \tag{2.34}$$

In such a universe, the age is actually estimated as

$$t_0 = \frac{2}{3}H_0^{-1} = 6.51h^{-1} \times 10^9 \ \ \text{years}. \tag{2.35}$$

Observational data from WMAP7 gives $h = 0.702$ [33], thus the age of the universe is estimated to be 9.27 Gyr. Carretta *et al.* [10] estimated the age of globular cluster in the Milky Way galaxy to be 12.9 ± 2.9 Gyr, whereas Jimenez *et al.* [27] found the value 13.5 ± 2 Gyr. Hansen et al. [20] constrained the age of globular cluster M4 to be 12.7 ± 0.7 Gyr. We see that, in most cases, the age of globular clusters are larger than 11 Gyr. Therefore the age of the universe estimated by Eq. (2.35) is inconsistent with the age of globular clusters mentioned above.

2.4.2 The age of the universe

In previous subsection, the cosmic age for dust model is inconsistence with the age of the globular clusters. However if dark energy term is included in Friedmann equation, the cosmic age problem can be resolved. Moreover the dark energy term can give accelerating universe. Now we consider in details. Consider Friedmann equation that includes dark energy term,

$$H^2 = \frac{8\pi G}{3}\left(\rho_{\rm r} + \rho_{\rm m} + \rho_{\rm DE}\right) - \frac{kc^2}{a^2}, \tag{2.36}$$

where $\rho_{\rm DE}$ is energy density for dark energy. The acceleration equation with dark energy term write

$$\frac{\ddot{a}}{a} = -\frac{4\pi G}{3}\left(\rho_{\rm r} + p_{\rm r} + \rho_{\rm m} + \rho_{\rm DE} + 3p_{\rm DE}\right). \tag{2.37}$$

This equation gives $\ddot{a} > 0$ if $p_{\rm DE} < -(\rho_{\rm r} + p_{\rm r} + \rho_{\rm m} + \rho_{\rm DE})/3$. Thus dark energy which possesses negative pressure can yield for accelerating universe. Now we turn our point to consider the term of dark energy. Assuming constant equation of state, Eq. (2.25) are written as

$$\rho_{\rm DE} = \rho_{\rm DE0}a^{-3(1+w_{\rm DE})}, \tag{2.38}$$

where $w_{\rm DE}$ is equation-of-state parameter of dark energy. In term of matter ($w_{\rm m} = 0$) and radiation ($w_{\rm rad} = 1/3$) we have $\rho_{\rm m} = \rho_{\rm m0}a^{-3}$ and $\rho_{\rm rad} = \rho_{\rm r0}a^{-4}$ respectively (we have set $a_0 \equiv 1$). Therefor the Friedmann equation becomes

$$H^2 = \frac{8\pi G}{3}\left[\rho_{\rm r0}a^{-4} + \rho_{\rm m0}a^{-3} + \rho_{\rm DE0}a^{-3(1+w_{\rm DE})}\right] - \frac{kc^2}{a^2}. \tag{2.39}$$

Writing the equation in term of density parameter and redshift z using relation (2.27), (2.30) and (2.23), the Friedmann equation reads

$$E(z) = \left[\Omega_{\rm r0}(1+z)^4 + \Omega_{\rm m0}(1+z)^3 + \Omega_{\rm DE0}(1+z)^{3(1+w_{\rm DE})} + \Omega_{k0}(1+z)^2\right]^{1/2}, \tag{2.40}$$

where $E(z) \equiv H(z)/H_0$. Using relation ${\rm d}t = -{\rm d}z/[(1+z)H]$, the age of the universe can be calculated via the equation

$$t_0 = \frac{1}{H_0}\int_0^\infty \frac{{\rm d}z}{E(z)(1+z)} \tag{2.41}$$

The expression (2.40) is dominated by the term of small redshift, thus for term of high redshift such radiation term can be neglected. Considering for simplest case, $w_{\rm DE} = -1$, Eq. (2.41) can be expressed as

$$t_0 = \frac{1}{H_0}\int_0^\infty \frac{{\rm d}z}{(1+z)\sqrt{\Omega_{\rm m0}(1+z)^3 + \Omega_{\rm DE0} + \Omega_{k0}(1+z)^2}}. \tag{2.42}$$

In case of flat universe, Eq. (2.42) is integrated to be

$$t_0 = \frac{1}{3H_0\sqrt{1-\Omega_{\rm m0}}} \ln\left(\frac{1+\sqrt{1-\Omega_{\rm m0}}}{1-\sqrt{1-\Omega_{\rm m0}}}\right), \tag{2.43}$$

where we have used $\Omega_{\rm m0} + \Omega_{\rm DE0} = 1$. The age of the universe is allowed to be

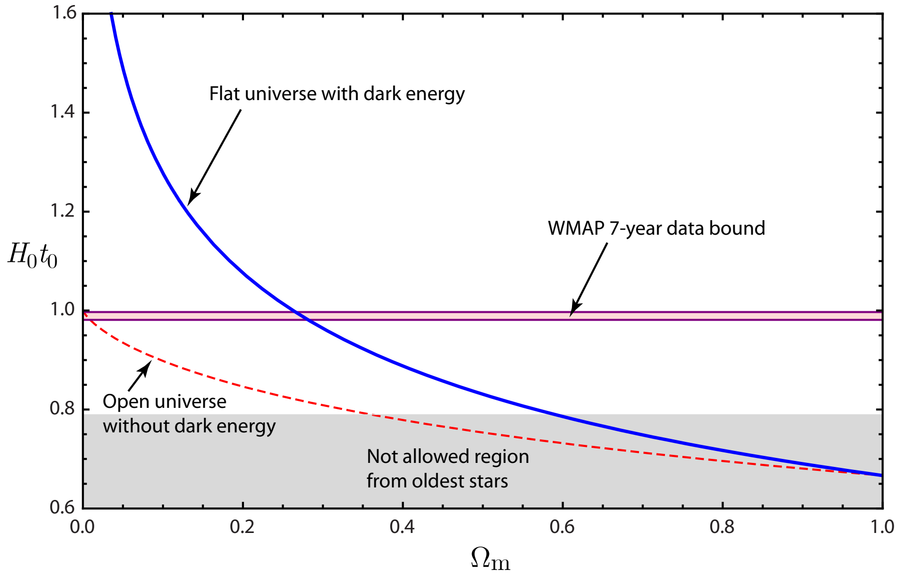

Figure 1. Plotting of the age of the universe and density parameter of matter shows that flat universe with dark energy (solid line) is consistent with WMAP 7-year bound. We see that the matter contributed in the universe is indeed about 28%, and dark energy is 72%

$t_0 > 11$ Gyr from observed the age of oldest stars. Thus we require that $0 > \Omega_{\rm m0} \geq 0.591$. The WMAP 7-year data (with $w_{\rm DE} = -1$) constraints the cosmic age to be 13.67 Gyr $\geq t_0 \geq$ 13.89 Gyr [33]. Therefore matter in the universe is constrained to be $0.265 \geq \Omega_{\rm m0} \geq 0.281$. This means that dark energy contributed in our universe amount 72% of the whole cosmic components.

For the open universe without dark energy the Eq. (2.42) becomes

$$t_0 = \frac{1}{H_0(1-\Omega_{\rm m0})}\left[1 + \frac{\Omega_{\rm m}}{2\sqrt{1-\Omega_{\rm m}}} \ln\left(\frac{1-\sqrt{1-\Omega_{\rm m0}}}{1+\sqrt{1-\Omega_{\rm m0}}}\right)\right], \tag{2.44}$$

where we have used $\Omega_{\rm m0}+\Omega_{k0} = 1$. Open universe without dark energy can not give the age of the universe larger than WMAP 7-year measurement (see Fig. 1). Thus in this case is inconsistence with observation. The discussions above show that the existence of dark energy is important to solve the cosmic age problem.

2.4.3 Accelerating universe and dark energy

In this subsection, we consider detail for accelerating universe. Upon the assumption flat-FLRW universe, $w_{\mathrm{DE}} = -1$ and neglecting radiation term, the Friedmann equation can be written as ($a_0 \equiv 1$)

$$H = \frac{\dot{a}}{a} = H_0 \left[\Omega_{\mathrm{m}} a^{-3} + \Omega_{\mathrm{DE}}\right]^{1/2}, \tag{2.45}$$

or in the integral form

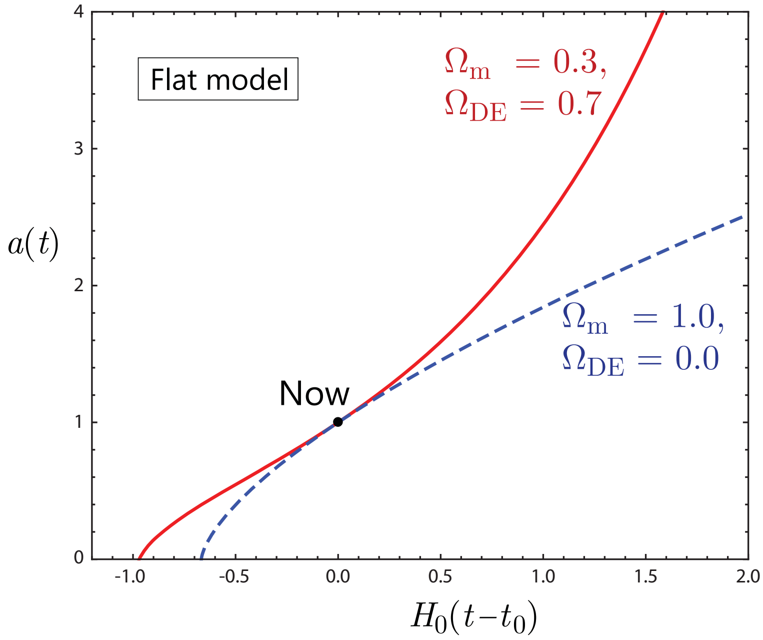

Figure 2. Plotting of the scale factor $a(t)$ versus $H_0(t-t_0)$ shows that the universe with dark energy (the solid line) gives accelerating expansion while dust model without dark energy (the dashed line) can not give accelerating universe.

$$H_0 \int_0^t \mathrm{d}t' = \int_0^a \frac{\mathrm{d}a'}{\sqrt{\Omega_{\mathrm{m}} a'^{-1} + \Omega_{\mathrm{DE}} a'^2}}. \tag{2.46}$$

Eq. (2.46) needs numerical calculation. For the universe without dark energy, Eq. (2.46) yields

$$a(t) = \left(\frac{3}{2}\sqrt{\Omega_{\mathrm{m}}} H_0 t\right)^{2/3}. \tag{2.47}$$

In Fig. 2 shows that the universe with dark energy (the solid line) gives accelerating expansion (obtain by Eq. (2.46)) while dust model without dark energy (the dashed line) can not give accelerating universe (obtain by Eq. (2.47)). This illustrates that accelerating universe problem can be solved by including the term of energy.

2.4.4 Type Ia Supernovae – observational evidence for dark energy

In 1998, Riess *et al.* [49] and Perlmutter *et al.* [48] indicate that the universe is under accelerating expansion. The cosmic acceleration is reported by observing luminosity distance of type Ia supernovae (SN Ia) which occurs when mass of a white dwarf exceeds Chandrasekhar limit [14] (about 1.38 Solar masses [41, 57]) in binary system.

If dark energy is included as a cosmic component. The luminosity distance will be large comparable to other measurements without dark energy. Let us consider the luminosity distance of a star defined as

$$d_{\mathrm{L}}^2 = \frac{L_{\mathrm{s}}}{4\pi F_{\mathrm{ob}}}, \tag{2.48}$$

where L_{s} is the light source's absolute luminosity and F_{ob} is an observed flux. Since the universe is expanding, the observed flux is then defined as a function of scale factor of the present time namely

$$F_{\mathrm{ob}} = \frac{L_{\mathrm{ob}}}{4\pi R^2(a_0)} = \frac{L_{\mathrm{ob}}}{4\pi \left(a_0 f_k(\chi)\right)^2}, \tag{2.49}$$

where L_{ob} is observed luminosity, and $R(a_0) = a_0 f_k(\chi)$ is distance from the receding star to the observer. Now the luminosity is taken as

$$d_{\mathrm{L}}^2 = \left(a_0 f_k(\chi)\right)^2 \frac{L_{\mathrm{s}}}{L_{\mathrm{ob}}}. \tag{2.50}$$

The luminosity is indeed an amount of energy per a time interval, $L_{\mathrm{s}} = \Delta\epsilon_{\mathrm{s}}/\Delta t_{\mathrm{s}}$, and also $L_{\mathrm{ob}} = \Delta\epsilon_{\mathrm{ob}}/\Delta t_{\mathrm{ob}}$. From Eq. (2.23), we have relation

$$1 + z = \frac{\nu_{\mathrm{s}}}{\nu_{\mathrm{ob}}} = \frac{\Delta\epsilon_{\mathrm{s}}}{\Delta\epsilon_{\mathrm{ob}}} = \frac{\Delta t_{\mathrm{ob}}}{\Delta t_{\mathrm{s}}} = \frac{a_0}{a}. \tag{2.51}$$

Thus the fraction $L_{\mathrm{s}}/L_{\mathrm{ob}}$ in Eq. (2.50) becomes

$$\frac{L_{\mathrm{s}}}{L_{\mathrm{ob}}} = \frac{\Delta\epsilon_{\mathrm{s}}}{\Delta t_{\mathrm{s}}}\frac{\Delta t_{\mathrm{ob}}}{\Delta\epsilon_{\mathrm{ob}}} = (1+z)^2. \tag{2.52}$$

Using Eq. (2.30) and Eq. (2.10) for non-flat universe, the luminosity distance becomes

$$d_{\mathrm{L}} = \frac{(1+z)c}{H_0\sqrt{\Omega_{k0}}}\sinh\left(\sqrt{-k}\chi\right). \tag{2.53}$$

The light ray traveling along χ direction satisfies $\mathrm{d}s^2 = c^2\mathrm{d}t^2 - a^2(t)\mathrm{d}\chi^2 = 0$, FLRW metric gives

$$\chi = \int_0^{\chi_{\mathrm{s}}} \mathrm{d}\chi = \int_{\mathrm{t_s}}^{t_{\mathrm{ob}}} \frac{c}{a(t)}\mathrm{d}t \tag{2.54}$$

Converting $t \to z$ by using the relation $\mathrm{d}t = -\mathrm{d}z/[(1+z)H]$, Eq. (2.54) becomes

$$\chi = \frac{c}{a_0 H_0}\int_0^z \frac{\mathrm{d}z'}{E(z')}, \tag{2.55}$$

where $E(z)$ is given by Eq. (2.40). Therefore luminosity distance expressed as function of redshift reads

$$d_{\mathrm{L}} = \frac{(1+z)c}{H_0\sqrt{\Omega_{k0}}}\sinh\left(\sqrt{\Omega_{k0}}\int_0^z \frac{\mathrm{d}z'}{E(z')}\right). \tag{2.56}$$

In case of flat universe, d_{L} can be expressed as

$$d_{\mathrm{L}} = \frac{(1+z)c}{H_0}\int_0^z \frac{\mathrm{d}z'}{E(z')}. \tag{2.57}$$

By assuming dark energy equation of state $w_{\mathrm{DE}} = -1$ and assuming flat universe, we have $E(z) = [\Omega_{\mathrm{m}0}(1+z)^3 + \Omega_{\mathrm{DE}0}]^{1/2}$. Thus the luminosity distance becomes

$$d_{\mathrm{L}} = \frac{(1+z)c}{H_0}\int_0^z \frac{\mathrm{d}z'}{\sqrt{\Omega_{\mathrm{m}0}(1+z')^3 + \Omega_{\mathrm{DE}0}}}, \tag{2.58}$$

which can be numerically evaluated for given $\Omega_{\mathrm{DE}0}$.

The apparent magnitude m of a star and its absolute magnitude M[2] is related to the luminosity distance d_{L} as

$$m - M = 5\log_{10} d_{\mathrm{L}} + 25, \tag{2.59}$$

where d_{L} is the luminosity distance of star in Magaparsec. In general, the absolute magnitude M of type Ia supernovae are nearly constant with little variation, which give $M = -19.30$ [22]. Because initial mass absorbed by white dwarf star is nearly

[2]absolute magnitude M is defined when distance d_{L} is equal to 10 parsec.

Chandrasekhar limit, that gives nearly constant absolute magnitude when they explode. Therefore the distance modulus μ_0 is often defined as $\mu_0 = m - M$, thus we can write

$$\mu_0 = 5\log_{10} d_{\rm L} + 25. \tag{2.60}$$

Measuring μ_0 of SN Ia gives also $d_{\rm L}$. Fig. (3) shows that observed $d_{\rm L}$ of 75 type

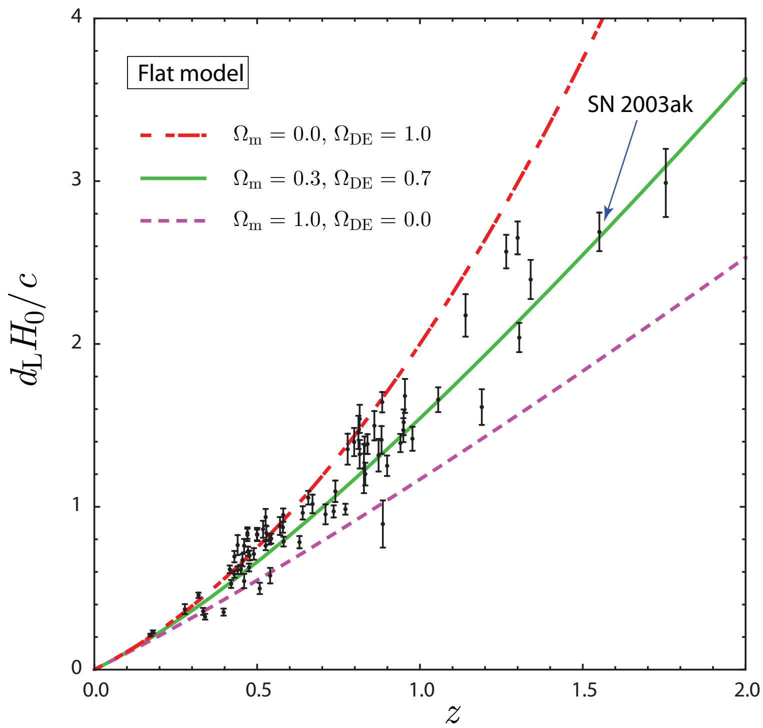

Figure 3. Plotting of the luminosity distance versus redshift of SN Ia for flat cosmological model. Most data from SN Ia correspond to $\Omega_{\rm DE} \simeq 0.7$ (the solid line).

Ia supernovae with their redshifts correspond to cosmological model with $\Omega_{\rm DE} = 0.7$. These SN Ia data are taken from the "Gold" data observed in the year 1997-2003 with $z > 0.1$ of report of Riess *et al.* [50] in 2004. For example for a datum, a distance modulus of supernova SN 2003ak is 45.30, which is evaluated via Eq. (2.60) to give $d_{\rm L} = 2.689$. Its observed redshift is 1.551, thus the supernova SN 2003ak corresponds $\Omega_{\rm DE} \simeq 0.7$ as shown in Fig. (3).

Riess *et al.* (2004) [50] reported the measurement of 16 high-redshift SN Ia with $z > 1.25$ by Hubble Space Telescope (HST). A best fitted value of $\Omega_{\rm m0}$ was found to be $\Omega_{\rm m0} = 0.29^{+0.05}_{-0.03}$ (1σ error). Figure 4 shows the observational values of the luminosity distance d_L versus redshift z. A best-fit value of Ω_{m0} obtained by Ref. [16] is $\Omega_{m0} = 0.31 \pm 0.08$, which is consistent with Riess *et al.*. This indicates that dark energy contributed in the universe is about 70%.

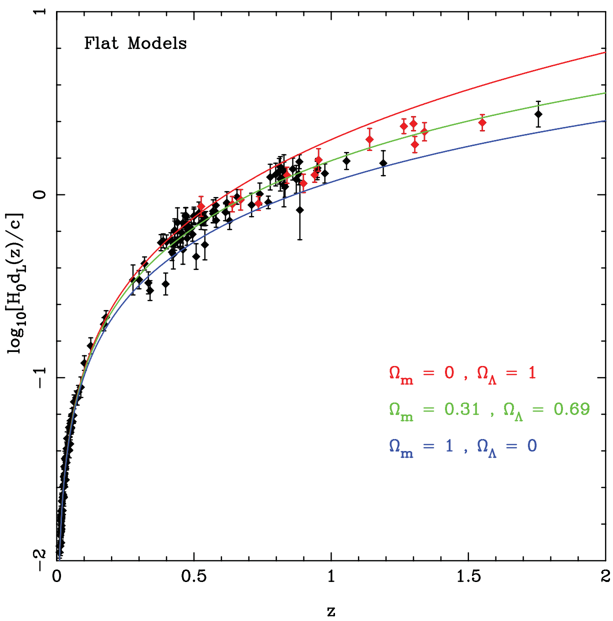

Figure 4. Plotting of the luminosity distance versus redshift for flat FLRW model. The black points are taken from the "Gold" dataset by Riess *et al.* [50], and the red points are taken from HST data measured in 2003. This Figure is taken from Ref. [16]

CHAPTER III

DARK ENERGY MODELS

Dark energy hypothesis is that there is some sort of energy permeating throughout space, and increases with the expansion of the universe [46]. It is the most accepted theory for explaining recent observations that the universe appears to be in accelerating expansion. In standard model of cosmology[3], dark energy currently accounts for 73% of total mass-energy of the universe.

In this Chapter (also later), we adopt natural units, such that $c = \hbar = 1$, where c is the speed of light and $\hbar$ is the reduced Planck's constant. We denote the Planck mass as $m_{\rm Pl} = G^{-1/2} = 1.22 \times 10^{19}$ GeV and reduced Planck mass as $M_{\rm Pl} = (8\pi G)^{-1/2} = 2.44 \times 10^{18}$ GeV. Finally, a constant κ is defined to be $\kappa \equiv \sqrt{8\pi G}$.

3.1 Cosmological constant

In 1917, Einstein included cosmological constant Λ in his field equations to attain a static universe. But it was dropped by him after Hubble's discovery of the expansion of the universe in 1929. In 1998, observations of Type Ia supernovae [48, 49] indicated that the expansion of the universe is accelerating. The cosmological constant was re-included in Einstein's field equations as a dark energy content for explaining this phenomenon. Many possible models of dark energy have been proposed such as quintessence, phantom field, but the cosmological constant is the simplest model of dark energy. In particle physics, the cosmological constant arises as an energy density of the vacuum. If it originates from the vacuum energy density, the energy scale of Λ is much larger than present Hubble constant H_0. This gives rise of *cosmological constant*

[3]Standard model of cosmology called ΛCDM model which is an abbreviation for Lambda-Cold Dark Matter. This model included cold dark matter model with dark energy, which is the simplest model in general agreement with observations.

problem [55].

3.1.1 Einstein's equations with cosmological constant

The Einstein's equations (2.11) satisfies Bianchi identities $\nabla_\mu G^{\mu\nu} = 0$ and momentum-energy conservation $\nabla_\mu T^{\mu\nu} = 0$. Since $\nabla_\alpha g^{\mu\nu} = 0$, a term $\Lambda g_{\mu\nu}$ can be included into the Einstein's equations. Therefore the Einstein's equations are written as

$$R_{\mu\nu} - \frac{1}{2} g_{\mu\nu} R = 8\pi G T_{\mu\nu} + \Lambda g_{\mu\nu}. \tag{3.1}$$

In the FLRW universe given by Eq. (2.8), the Einstein equations (3.1) give

$$H^2 = \frac{8\pi G}{3}\rho - \frac{k}{a^2} + \frac{\Lambda}{3} \tag{3.2}$$

$$\frac{\ddot{a}}{a} = -\frac{4\pi G}{3}(\rho + 3p) + \frac{\Lambda}{3}. \tag{3.3}$$

By using the field equations (3.2) and (3.3) with dust-dominated universe ($p = 0$), the Einstein's static universe, $H = 0$, corresponds to

$$\rho = \frac{\Lambda}{4\pi G}, \quad \frac{k}{a^2} = \Lambda\,. \tag{3.4}$$

Since ρ is positive, and also Λ is required to be positive. This means that the static universe corresponds to $k = +1$. However the static universe was abnegated due to discovery of expanding universe. However it returned again in the late 1990's to explain the observed acceleration of the universe. Introducing the modified energy density and pressure as the form

$$\tilde{\rho} = \rho + \rho_\Lambda, \tag{3.5}$$

$$\tilde{p} = p + p_\Lambda, \tag{3.6}$$

where $\rho_\Lambda \equiv \Lambda/8\pi G$ and $p_\Lambda \equiv -\Lambda/8\pi G$. From the expressions above, the Eqs. (3.2) and (3.3) reduce to the Friedmann equations Eqs. (2.18) and (2.17). Note that equation-of-state parameter of cosmological constant is given by $w_\Lambda \equiv p_\Lambda/\rho_\Lambda = -1$.

3.1.2 Vacuum energy and fine-tuning problem

If the cosmological constant Λ dominates universe, hence from Eq. (3.2), the value of Λ ought to be of order the present value of the Hubble parameter H_0, that is [2, 17, 46, 55]

$$\Lambda \approx H_0^2. \tag{3.7}$$

Therefore the density of Λ is approximated in the order

$$\rho_\Lambda = \frac{\Lambda}{8\pi G} \approx 10^{-47}\,\mathrm{GeV}^4\,. \tag{3.8}$$

If cosmological constant originates from vacuum energy, this is a serious problem because vacuum energy scale is much difference from the dark energy density observed today [55]. The vacuum energy can be evaluated by the sum of lowest possible energy E_0, zero-point energy of quantum harmonic oscillators with mass m, given by

$$E_0 = \sum_i \frac{1}{2}\omega_i \quad \rightarrow \quad \frac{1}{2}\int \omega_{\mathbf{k}} D(\mathbf{k})\mathrm{d}^3\mathbf{k}, \tag{3.9}$$

where we integrate over all wave vectors $\mathbf{k}$, and $D(\mathbf{k})$ is density of mode. Putting the system in a box of volume L^3, and impose periodic boundary conditions, we have $D(\mathbf{k}) = L^3/(2\pi)^3$. Therefore Eq. (3.9) becomes

$$E_0 = \frac{L^3}{2}\int \frac{\omega_{\mathbf{k}}}{(2\pi)^3}\mathrm{d}^3\mathbf{k}. \tag{3.10}$$

The energy density of vacuum ρ_{vac} can be obtained by taking $L \rightarrow \infty$. Using $\omega_{\mathbf{k}}^2 = k^2 + m^2$, we have

$$\begin{aligned} \rho_{\mathrm{vac}} &= \lim_{L\to\infty} \frac{E_0}{L^3} \\ &= \lim_{L\to\infty} \frac{L^3}{2L^3}\int_0^{k_{\mathrm{max}}} \frac{\sqrt{k^2+m^2}}{(2\pi)^3}\mathrm{d}^3\mathbf{k} \\ &= \frac{1}{4\pi^2}\int_0^{k_{\mathrm{max}}} \mathrm{d}k\, k^2\sqrt{k^2+m^2}. \end{aligned} \tag{3.11}$$

If we impose a cut-off at a maximum wave vector $k_{\mathrm{max}} \gg m$, we obtain [13, 46, 55]

$$\rho_{\mathrm{vac}} \approx \frac{k_{\mathrm{max}}^4}{16\pi^2}. \tag{3.12}$$

If general relativity is still valid up to Planck scale, and hence taking $k_{\text{max}} = m_{\text{pl}}$, we obtain the vacuum energy density as

$$\rho_{\text{vac}} \approx 10^{74}\,\text{GeV}^4. \tag{3.13}$$

This value is larger than the observed value given by Eq. (3.8) about 121 orders of magnitude. This is a fine-tuning problem which requires a fine adjustment of ρ_Λ to the observed energy density of the universe today. However, the large discrepancy is not yet explained.

3.2 Scalar field models of dark energy

Cosmological constant model in the previous subsection gives constant of equation-of-state parameter $w_\Lambda = -1$. Nowadays, the observed value of w is close to -1 and it has a little time variation. This situation leads to considering dynamical dark energy equation of state. Scalar field ϕ is motivated from particle physics for describing flatness problem and horizon problem in inflationary universe model, which was proposed by Guth in 1981 [19]. Particle physics models suggest that existence of scalar field ϕ is needed in symmetry breaking mechanism. Scalar field driving inflation is called inflaton field. Now the scalar field is a model of dark energy with time-dependent equation of state. In this section we roughly discuss about homogeneous scalar field ($\phi = \phi(t)$), which included quintessence field, phantom field, k-essence field and Dirac-Born-Infeld dark energy.

3.2.1 Quintessence field

Cosmological model of dark energy which is a canonical scalar field ϕ is called "quintessence" [8, 58]. This scalar field is similar to that of inflation, but it gives rate of expansion of the universe much slower than inflation. The action for quintessence is given by [17, 46]

$$S = \int \left[\frac{1}{2}g^{\mu\nu}\partial_\mu\phi\partial_\nu\phi - V(\phi)\right]\sqrt{-g}\;\mathrm{d}^4x, \tag{3.14}$$

where ϕ is the quintessence field with potential $V(\phi)$, and g is determinant of $g_{\mu\nu}$.

Variation of the action (3.14) with respect to ϕ gives

$$\frac{\delta S}{\delta \phi} \equiv 0 = \sqrt{-g}\, g^{\mu\nu}\partial_\mu\partial_\nu\phi + g^{\mu\nu}\partial_\nu\phi\,\partial_\mu\sqrt{-g} + \sqrt{-g}\,\frac{\mathrm{d}V}{\mathrm{d}\phi}. \tag{3.15}$$

In flat FLRW background ($k = 0$), the metric (2.8) gives $\sqrt{-g} = a^3$. Then considering for only homogeneous field, we find

$$\ddot{\phi} + 3H\dot{\phi} + V_{,\phi} = 0, \tag{3.16}$$

where $V_{,\phi} \equiv \mathrm{d}V/\mathrm{d}\phi$.

The energy momentum tensor of the scalar field can be derived by varying the action (3.14) respects to the metric $g^{\mu\nu}$ as in the form

$$T_{\mu\nu} = \frac{2}{\sqrt{-g}}\frac{\delta S}{\delta g^{\mu\nu}}. \tag{3.17}$$

Note that $\delta\sqrt{-g} = -(1/2)\sqrt{-g}g_{\mu\nu}\delta g^{\mu\nu}$, then the energy momentum tensor is taken the form

$$T_{\mu\nu} = \partial_\mu\phi\,\partial_\nu\phi - g_{\mu\nu}\left[\frac{1}{2}g^{\rho\sigma}\partial_\rho\phi\,\partial_\sigma\phi + V(\phi)\right]. \tag{3.18}$$

Energy density and pressure of the scalar field can be found by

$$\rho_\phi = T^0_0 = \frac{1}{2}\dot{\phi}^2 + V(\phi), \tag{3.19}$$

$$p_\phi = -T^i_i = \frac{1}{2}\dot{\phi}^2 - V(\phi). \tag{3.20}$$

Then the Friedmann equation (2.18) and acceleration equation (2.17) yield

$$H^2 = \frac{\kappa^2}{3}\left[\frac{1}{2}\dot{\phi}^2 + V(\phi)\right], \tag{3.21}$$

$$\frac{\ddot{a}}{a} = -\frac{\kappa^2}{3}\left[\dot{\phi}^2 - V(\phi)\right]. \tag{3.22}$$

Hence accelerating expansion of the universe ($\ddot{a} > 0$) occurs when $\dot{\phi}^2 < V(\phi)$. The equation of state for the field ϕ is given by

$$w_\phi \equiv \frac{p}{\rho} = \frac{\dot{\phi}^2 - 2V(\phi)}{\dot{\phi}^2 + 2V(\phi)}. \tag{3.23}$$

In case of $\dot{\phi}^2 \ll V(\phi)$ and $\ddot{\phi} \simeq 0$, Eq. (3.16) and (3.22) give the approximation

$$3H\dot{\phi} \simeq -V_{,\phi} \quad \text{and} \quad 3H^2 \simeq \kappa^2 V(\phi),$$

respectively. Hence the equation-of-state parameter Eq. (3.23) can be approximated to

$$w_\phi \simeq -1 + \frac{2}{3}\epsilon, \tag{3.24}$$

where $\epsilon \equiv (V_{,\phi}/V)^2/(2\kappa^2)$ is called slow-roll parameter [37].

The fluid equation of the field is taken the form

$$\dot{\rho}_\phi + 3H(1+w_\phi)\rho_\phi = 0, \tag{3.25}$$

which can be written in an integrated form:

$$\rho = \rho_0 \exp\left[-\int 3(1+w_\phi)\frac{\mathrm{d}a}{a}\right], \tag{3.26}$$

where ρ_0 is an integration constant. The Eq. (3.23) implies that w_ϕ ranges in the region $-1 \leq w_\phi \leq 1$. The limit $\dot{\phi}^2 \ll V(\phi)$ corresponds to $w_\phi = -1$, which gives constant ρ from Eq. (3.26). In the case $\dot{\phi}^2 \gg V(\phi)$ gives $w_\phi = 1$, and hence $\rho \propto a^{-6}$ as Eq. (3.26). In other cases, the behavior of the evolution of energy density with scale factor is presumed that obeys

$$\rho \propto a^{-m}, \quad 0 < m < 6. \tag{3.27}$$

Hence $w_\phi < -1/3$ or $0 \leq m < 2$ yields the accelerating expansion of the universe (as seen from Eq. (2.17)). From the solution (2.26), It suggests to write the scale factor as a function of power law exponent of time

$$a(t) \propto t^\beta, \tag{3.28}$$

with the accelerated expansion occurs for $\beta > 1$. The acceleration equation (2.17) for quintessence field gives $\dot{H} = -4\pi G\dot{\phi}^2$. Therefore the potential $V(\phi)$ the scalar field ϕ can be expressed, respectively, as

$$V = \frac{3H^2}{8\pi G}\left(1 + \frac{\dot{H}}{3H^2}\right), \tag{3.29}$$

$$\phi = \int \mathrm{d}t\left(-\frac{\dot{H}}{4\pi G}\right)^{1/2}. \tag{3.30}$$

One of the problems of quintessence field is that it could couple to ordinary matter. This leads to long range forces and time dependence of physical constants [11].

3.2.2 Phantom field

The quintessence field models discussed in the previous subsection correspond to equation-of-state parameter $w \geq -1$. When $w < -1$, the model is of phantom type. Indeed observation today indicates that the equation-of-state parameter lies in a narrow region around $w = -1$ [33]. Simplest model of phantom dark energy is provided by negative kinetic term of scalar field [7, 12]. The action of the phantom field is given by

$$S = \int \left[-\frac{1}{2} g^{\mu\nu} \partial_\mu \phi \partial_\nu \phi - V(\phi) \right] \sqrt{-g} \, \mathrm{d}^4 x. \tag{3.31}$$

Similar method to the case of quintessence, the equation of motion for the phantom field is then given by

$$\ddot{\phi} + 3H\dot{\phi} = V_{,\phi}. \tag{3.32}$$

The evolution of Eq. (3.32) is the same as that of the normal scalar field but the negative kinetic energy of the field allows it to evolve from lower value to higher potential [52]. The energy density and pressure density for phantom field can be found, respectively, from the Eq. (3.17), which is given by

$$\rho_\phi = -\frac{\dot{\phi}^2}{2} + V(\phi), \tag{3.33}$$

$$p_\phi = -\frac{\dot{\phi}^2}{2} - V(\phi). \tag{3.34}$$

Since the energy density is positive by definition therefore $\dot{\phi}^2/2 < V(\phi)$ which gives accelerating expansion. The equation of state of the phantom field is taken form

$$w_\phi = \frac{p_\phi}{\rho_\phi} = \frac{\dot{\phi}^2 + 2V(\phi)}{\dot{\phi}^2 - 2V(\phi)} \tag{3.35}$$

which allowing value of w_ϕ lies in region $-\infty < w_\phi \leq -1$. Note that the evolution of scale factor Eq. (2.26) corresponds to contracting universe for $w < -1$. Therefore, for phantom field, the scale factor Eq. (2.26) must be slightly modified to be

$$a(t) \propto (t_\mathrm{s} - t)^\beta, \tag{3.36}$$

where $\beta \equiv 2/3(1 + w_\phi) < 0$, and t_s is constant with $t_\mathrm{s} > t$. The Hubble parameter is then taken the form

$$H = -\frac{\beta}{t_\mathrm{s} - t}. \tag{3.37}$$

Note that the Hubble parameter diverges as $t \to t_{\rm s}$. Moreover, the scalar curvature also grows to in infinity as $t \to t_{\rm s}$ [17]. These correspond to big rip singularity in the future [9].

3.2.3 Tachyon field

Tachyons are a class of particles which is able to travel faster than the speed of light. Tachyon has strange property, i.e. when increasing velocity, its energy decreases. The slowest speed for tachyons is the speed of light. Consider a normal relativistic particle with energy-momentum relation $E^2 = p^2 + m^2$, the total energy of the particle with velocity v is given by

$$E = \frac{m}{\sqrt{1 - v^2}}.$$

If $v > 1$ then the above equation give imaginary energy. For describing tachyons with real masses, we must treats $m = iz$, where $i = \sqrt{-1}$. Therefore energy-momentum relation and the total energy become

$$E^2 + z^2 = p^2, \qquad E = \frac{z}{\sqrt{v^2 - 1}}. \tag{3.38}$$

The above equation implies that the energy of tachyon decreases when its velocity increases. In relativistic mechanics, relativistic particle with position $q(t)$ and mass m is described by Lagrangian $L = -m\sqrt{1 - \dot{q}^2}$ [45]. In view point of field theory, the mass m is treated as a function of scalar field ϕ, namely $V(\phi)$. Therefore the action for homogeneous tachyon field is taken form [5]

$$S = \int \left[-V(\phi)\sqrt{1 - g^{\mu\nu}\partial_\mu\phi\partial_\nu\phi} \right] \mathrm{d}^4x, \tag{3.39}$$

where $V(\phi)$ is treated as potential of the field. In a flat FRW background the energy density ρ and the pressure density p for the tachyon field are given by

$$\rho_{\rm tach} = \frac{V(\phi)}{\sqrt{1 - \dot{\phi}^2}}, \qquad p_{\rm tach} = -V(\phi)\sqrt{1 - \dot{\phi}^2}. \tag{3.40}$$

Then equation of state is given by

$$w_{\rm tach} = \dot{\phi}^2 - 1. \tag{3.41}$$

Hence from Eq. (2.17), the accelerating expansion of the universe occurs when $\dot{\phi}^2 < 2/3$. However, if tachyons were conventional that move faster than speed light ($\dot{\phi} > 1$), this would leads to violations of causality in special relativity, and this yields the contracting universe.

3.2.4 Other models

There are many other models of single-scalar field dark energy which we do not consider here, such as K-essence field, Dirac-Born-Infeld (DBI) dark energy.

The k-essence models was found rely on dynamical attractor properties of scalar fields with nonlinear kinetic energy terms in the action [4] k-essence is characterized by a scalar field with non-canonical kinetic energy. The Lagrangian for k-essence corresponds to a pressure which is a function of scalar field and its derivative [3, 4, 15]. A shortcoming of this model is that it needs to adjust energy scale to be order of the present energy density of the universe [17].

Another one is Dirac-Born-Infeld (DBI) dark energy. The DBI action motivated from string theory provides new classes of dark energy due to its relativistic kinematics [1]. Serious shortcoming of DBI model is, for simple potentials, the equation-of-state parameter appears to be too far from the present observation [40].

CHAPTER IV

PHANTOM POWER-LAW COSMOLOGY

In this work we desire to impose observational constraints on phantom power-law cosmology, that is on the scenario of a phantom scalar field along with the matter fluid in which the scale factor is a power law. In particular, we use cosmological observations from Cosmic Microwave Background (CMB), Baryon Acoustic Oscillations (BAO) and observational Hubble data (H_0), in order to impose complete constraints on the model parameters, focusing on the power-law exponent and on the big rip time.

In section 4.1 we construct the scenario of phantom power-law cosmology. In section 4.2 we use observational data in order to impose constraints on the model parameters. Finally, in section 4.3 we discuss the physical implications of the obtained results.

4.1 Phantom cosmology with power-law expansion

In this section we present phantom cosmology under power-law expansion. Matter contributed in the universe we consider here is baryonic matter plus cold dark matter, which is assumed to be a barotropic fluid with energy density $\rho_{\rm m}$ and pressure $p_{\rm m}$, and equation-of-state parameter $w_{\rm m} = p_{\rm m}/\rho_{\rm m}$. Since we focus on small redshifts, the radiation sector is neglected, thus the Friedmann equation and acceleration equation with phantom energy write:

$$\begin{aligned} H^2 &= \frac{8\pi G}{3}\left(\rho_{\rm m}+\rho_{\phi}\right)-\frac{k}{a^2} && (4.1)\\ \frac{\ddot{a}}{a} &= -\frac{4\pi G}{3}\left(\rho_{\rm m}+\rho_{\phi}+3p_{\rm m}+3p_{\phi}\right) && (4.2)\end{aligned}$$

The helpful relation for calculate the phantom potential is to express Eq. (4.1) and (4.2) in the term of $\dot{H}$, namely

$$\dot{H}=\frac{\ddot{a}}{a}-\frac{\dot{a}^2}{a^2}=-4\pi G\left(\rho_{\rm m}+p_{\rm m}+\rho_{\phi}+p_{\phi}\right)+\frac{k}{a^2}. \qquad (4.3)$$

In these expressions, ρ_ϕ and p_ϕ are respectively the energy density and pressure of the phantom field, which are given by Eq. (3.33) and Eq. (3.34).

We note that in phantom cosmology the dark energy sector is attributed to the phantom field, that is $\rho_{\rm DE} \equiv \rho_\phi$ and $p_{\rm DE} \equiv p_\phi$, and thus its equation-of-state parameter is given by

$$w_{\rm DE} \equiv \frac{p_{\rm DE}}{\rho_{\rm DE}} = \frac{p_\phi}{\rho_\phi}. \tag{4.4}$$

Considering the solution of fluid equation for matter Eq. (2.25) which is written as

$$\rho_{\rm m} = \frac{\rho_{\rm m0}}{a^n}, \tag{4.5}$$

where $n \equiv 3(1 + w_{\rm m})$ and $\rho_{\rm m0} \geq 0$ is the value at present time t_0.

Lastly, we can extract two helpful relations, by rearranging (4.1) we obtain

$$\begin{aligned} \rho_\phi &= \frac{3}{\kappa^2}\left(H^2 - \frac{\kappa^2}{3}\rho_{\rm m} + \frac{k}{a^2}\right) \\ &= \frac{3}{\kappa^2}\left(H^2 - \frac{\kappa^2}{3}\frac{\rho_{\rm m0}}{a^n} + \frac{k}{a^2}\right), \end{aligned} \tag{4.6}$$

while substitution of Eq. (3.33) and (3.34) into Eq. (4.3) gives

$$\begin{aligned} \dot\phi^2 &= \frac{2}{\kappa^2}\left(\dot H - \frac{k}{a^2}\right) + \rho_{\rm m}\frac{n}{3} \\ &= \frac{2}{\kappa^2}\left(\dot H - \frac{k}{a^2}\right) + \frac{n}{3}\frac{\rho_{\rm m0}}{a^n}, \end{aligned} \tag{4.7}$$

Note that $\kappa \equiv \sqrt{8\pi G}$, as we introduced in the Chapter 3.

Since we study the power-law behavior of the scale factor in phantom cosmology, then we use Eq. (3.36) to model the expansion of the universe. The scale factor takes the form [42, 43]

$$a(t) = a_0\left(\frac{t_{\rm s} - t}{t_{\rm s} - t_0}\right)^\beta, \tag{4.8}$$

with a_0 the value of the scale factor at present time t_0, while the Hubble parameter and its time derivative read:

$$H(t) \equiv \frac{\dot a(t)}{a(t)} = -\frac{\beta}{t_{\rm s} - t} \tag{4.9}$$

$$\dot H = -\frac{\beta}{(t_{\rm s} - t)^2}. \tag{4.10}$$

Since $\beta < 0$ we have an accelerating ($\ddot{a}(t) > 0$) and expanding ($\dot{a}(t) > 0$) universe, which possesses a positive $\dot{H}(t)$ that is it exhibits super-acceleration [18, 30].

In section 3.2.2, we have an un-determine phantom potential $V(\phi)$ and a phantom scalar field ϕ, which come from scalar field theory. Now we have more sufficiently helpful relations to reconstruct the phantom potential and the phantom scalar field by observational data. Thus by substituting Eq. (4.6) and (4.7) into Eq. (3.33), we obtain the phantom potential

$$V(\phi) = \frac{3}{8\pi G}\left(H^2 + \frac{\dot{H}}{3} + \frac{2k}{3a^2}\right) + \left(\frac{n-6}{6}\right)\frac{\rho_{\mathrm{m0}}}{a^n}. \tag{4.11}$$

In the following we consider as usual the matter (dark matter plus baryonic matter) component to be dust, that is $w_{\mathrm{m}} \approx 0$ or equivalently $n = 3$. Thus, using the Eq. (4.8), restoring the SI units and using also $M_{\mathrm{P}}^2 = \hbar c/\kappa^2$, we find

$$V(t) = \frac{M_{\mathrm{P}}^2 c}{\hbar}\left[\frac{3\beta^2 - \beta}{(t_{\mathrm{s}} - t)^2} + \frac{2kc^2(t_{\mathrm{s}} - t_0)^{2\beta}}{a_0^2(t_{\mathrm{s}} - t)^{2\beta}}\right] - \frac{\rho_{\mathrm{m0}}c^2}{2}\frac{(t_{\mathrm{s}} - t_0)^{3\beta}}{a_0^3(t_{\mathrm{s}} - t)^{3\beta}}. \tag{4.12}$$

Additionally, solving Eq. (4.7) by using Eq. (4.10) for the phantom field and inserting the power-law scale factor, gives

$$\phi(t) = \int\sqrt{\frac{2M_{\mathrm{P}}^2 c}{\hbar}\left[-\frac{\beta}{(t_{\mathrm{s}} - t)^2} - \frac{kc^2(t_{\mathrm{s}} - t_0)^{2\beta}}{a_0^2(t_{\mathrm{s}} - t)^{2\beta}}\right] + \frac{\rho_{\mathrm{m0}}c^2(t_{\mathrm{s}} - t_0)^{3\beta}}{a_0^3(t_{\mathrm{s}} - t)^{3\beta}}}\,\mathrm{d}t. \tag{4.13}$$

Finally, the time-dependence of the phantom energy density and pressure can be extracted from Eq. (3.33) and (3.34) by using Eq. (4.12) and (4.13), namely

$$\rho_\phi = \frac{M_{\mathrm{P}}^2 c}{\hbar}\left[\frac{3\beta^2}{(t_{\mathrm{s}} - t)^2} + \frac{3kc^2(t_{\mathrm{s}} - t_0)^{2\beta}}{a_0^2(t_{\mathrm{s}} - t)^{2\beta}}\right] - \frac{\rho_{\mathrm{m0}}c^2(t_{\mathrm{s}} - t_0)^{3\beta}}{a_0^3(t_{\mathrm{s}} - t)^{3\beta}}, \tag{4.14}$$

$$p_\phi = -\frac{M_{\mathrm{P}}^2 c}{\hbar}\left[\frac{3\beta^2 - 3\beta}{(t_{\mathrm{s}} - t)^2}\right] - \frac{\rho_{\mathrm{m0}}c^2(t_{\mathrm{s}} - t_0)^{3\beta}}{2a_0^3(t_{\mathrm{s}} - t)^{3\beta}}. \tag{4.15}$$

Note that at $t \to t_{\mathrm{s}}$, ρ_ϕ and p_ϕ diverge. However w_{DE} remains finite. This is exactly the big rip behavior according to the classification of singularities of [17, 44].

All the aforementioned can be expressed in terms of the redshift z. In particular, since $1 + z = a_0/a$, in phantom power-law cosmology we have

$$1 + z = \left(\frac{t_{\mathrm{s}} - t_0}{t_{\mathrm{s}} - t}\right)^\beta. \tag{4.16}$$

Therefore, using this relation we can extract the z-dependence of all the relevant quantities of the scenario, which can then straightforwardly be confronted by the data.

4.2 Observational constraints

In the present section we can proceed to confrontation with observations. In particular, we use Cosmic Microwave Background (CMB), Baryon Acoustic Oscillations (BAO) and Observational Hubble Data (H_0), in order to impose constraints on the model parameters, and especially to the power-law exponent β and to the Big Rip time t_s. Finally, we first obtain our results using only the CMB-WMAP7 data [35], and then we perform a combined fit using additionally the BAO [47] and H_0 ones [51, 54].

In this work we prefer not to use SNIa data as in the combined WMAP5+BAO +SNIa dataset [32]. This is because the combined WMAP5 with SNIa data from [21, 34] do not include systematic error, and the cosmological parameter derived from the combined WMAP5 dataset also differ from derivation of SNIa data [31]. Inclusion of the SNIa systematic error, which is comparable with its statistical error, can significantly alter the value of equation-of-state parameter [33]. Furthermore the value of equation-of-state parameter derived from two different light-curve fitters are different [6]. This could make it difficult to identify if w_DE is phantom case.

Firstly, we consider the power-law exponent β in the present time, which can be expressed as

$$\beta = -H_0(t_\mathrm{s} - t_0). \tag{4.17}$$

In a general, non-flat geometry the big rip time t_s cannot be calculated, bringing a large uncertainty to the observational fitting. However, one could estimate it by assuming a flat geometry, which is a very good approximation [33]. This is a very plausible assumptions [9]. Considering Friedmann equation for $k = 0$, which include dark energy term,

$$H^2 \equiv \left(\frac{\dot{a}}{a}\right)^2 = H_0^2 \left(\frac{\rho_\mathrm{m}}{\rho_{c0}} + \frac{\rho_\mathrm{DE}}{\rho_{c0}}\right), \tag{4.18}$$

where the subscripts “0” stand for value at the present time. We assume the evolution of phantom dark energy obeys Eq. (3.25), which its solution is then taking the integral form as shown in Eq. (3.26). However for constant equation-of-state parameter, Eq. (3.26) yields

$$\rho_{\rm DE} = \rho_{\rm DE0} a^{-3(1+w_{\rm DE})}. \tag{4.19}$$

We have $\rho_{\rm m} = \rho_{\rm m0} a^{-3}$, as shown in Eq. (4.5) for $n = 3$, then the Eq. (4.18) becomes

$$\frac{\dot{a}}{a} = H_0 \left(\frac{\Omega_{\rm m0}}{a^3} + \frac{\Omega_{\rm DE0}}{a^{3(1+w_{\rm DE})}} \right)^{1/2}, \tag{4.20}$$

The universe today is already dark-energy-dominated, thus the matter term in Eq. (4.20) can be neglected. With $\Omega_k = 0$, we have $\Omega_{\rm DE0} = 1 - \Omega_{\rm m0}$, then Eq. (4.20) becomes

$$\int_{a_0}^{\infty} a^{3(1+w_{\rm DE})/2-1} {\rm d}a = \int_{t_0}^{t_{\rm s}} H_0 (1-\Omega_0)^{1/2} {\rm d}t, \tag{4.21}$$

where $t_{\rm s}$ is big rip time, time at $a \to \infty$. Integrating equation above with rescale $a_0 \equiv 1$, $t_{\rm s}$ can be expressed as [9]

$$t_{\rm s} \simeq t_0 + \frac{2}{3} |1 + w_{\rm DE}|^{-1} H_0^{-1} (1 - \Omega_{\rm m0})^{-1/2}. \tag{4.22}$$

We have all the required information, and now we proceed to the data fitting. For the case of the WMAP7 data alone we use the maximum likelihood parameter values for H_0, t_0, $\Omega_{\rm CDM0}$ and $\Omega_{\rm b0}$ [33], focusing on the flat geometry. Additionally, we perform a combined observational fitting, using WMAP7 data, along with Baryon Acoustic Oscillations (BAO) in the distribution of galaxies, and Observational Hubble Data (H_0).

4.3 Results and discussions

In the previous section we presented the method that allows for the confrontation of power-law phantom cosmology with the observational data. In the present section we perform such an observational fitting, presenting our results, and discussing their physical implications.

First of all, in Table 2, we show for completeness the maximum likelihood values for the present time t_0, the present Hubble parameter H_0, the present baryon density parameter $\Omega_{\rm b0}$ and the present cold dark matter density parameter $\Omega_{\rm CDM0}$, that was used in our fitting [33], in WMAP7 as well as in the combined fitting. In fact, fitting parameters are obtained from maximum likelihood values, whereas the error bars are extracted from mean values. Realizing that both maximum likelihood values and mean values have the same distribution function.

We use equation-of-state parameter $w_{\rm DE}$ from WMAP7-year data which is $w_{\rm DE} = -1.12$ [35] to calculate the big rip time $t_{\rm s}$ via Eq. (4.22) without including error bar of $w_{\rm DE}$. Including error bar in $w_{\rm DE}$ can dramatic changes the value of $t_{\rm s}$ (See detail in Appendix A). In the same table we also provide the 1σ bounds of every parameter.

Parameter	**WMAP7+BAO+H_0**	**WMAP7**
t_0	13.78 ± 0.11 Gyr	13.71 ± 0.13 Gyr
	$[(4.33 \pm 0.04) \times 10^{17}$ sec]	$[(4.32 \pm 0.04) \times 10^{17}$ sec]
H_0	$70.2^{+1.3}_{-1.4}$ km/s/Mpc	71.4 ± 2.5 km/s/Mpc
$\Omega_{\rm b0}$	0.0455 ± 0.0016	0.0445 ± 0.0028
$\Omega_{\rm CDM0}$	0.227 ± 0.014	0.217 ± 0.026

Table 2. The maximum likelihood values in 1σ confidence level for the present time t_0, the present Hubble parameter H_0, the present baryon density parameter $\Omega_{\rm b0}$ and the present cold dark matter density parameter $\Omega_{\rm CDM0}$, for WMAP7 as well as for the combined fitting WMAP7+BAO+H_0. The values are taken from [33].

In Table 3 we present the maximum likelihood values and the 1σ bounds for the derived parameters, namely the power-law exponent β, the present matter energy density value $\rho_{\rm m0}$, the present critical energy density value $\rho_{\rm c0}$ and the big rip time $t_{\rm s}$.

Let us discuss in more detail the values and the evolution of some quantities of interest. For the combined data WMAP7+BAO+H_0, the potential Eq. (4.12) is fitted as

$$V(t) \approx \frac{6.47 \times 10^{27}}{(3.30 \times 10^{18} - t)^2} - 2.51 \times 10^{-371}(3.30 \times 10^{18} - t)^{19.54}, \tag{4.23}$$

while WMAP7 data alone give

$$V(t) \approx \frac{6.37 \times 10^{27}}{(3.23 \times 10^{18} - t)^2} - 1.99 \times 10^{-368}(3.23 \times 10^{18} - t)^{19.39}. \tag{4.24}$$

Parameter	WMAP7+BAO+H_0	WMAP7
β	$-6.51^{+0.24}_{-0.25}$	-6.5 ± 0.4
$\rho_{\rm m0}$	$(2.52 \pm 0.26) \times 10^{-27}$ kg/m^3	$(2.50 \pm 0.30) \times 10^{-27}$ kg/m^3
$\rho_{\rm c0}$	$(9.3^{+0.3}_{-0.4}) \times 10^{-27}$ kg/m^3	$(9.57 \pm 0.67) \times 10^{-27}$ kg/m^3
$t_{\rm s}$	$104.5^{+1.9}_{-2.0}$ Gyr	102.3 ± 3.5 Gyr
	$[(3.30 \pm 0.06) \times 10^{18}$ sec$]$	$[(3.23 \pm 0.11) \times 10^{18}$ sec$]$

Table 3. Derived maximum likelihood values in 1σ confidence level for the power-law exponent β, the present matter energy density value $\rho_{\rm m0}$, the present critical energy density value $\rho_{\rm c0}$ and the big rip time $t_{\rm s}$, for WMAP7 as well as for the combined fitting WMAP7+BAO+H_0.

Note that the second terms in these expressions, although very small at early times, they become significant at late times, that is close to the big rip. In particular, the inflection happens at $22.4^{+1.9}_{-2.0}$ Gyr (WMAP7+BAO+H_0) and 22.0 ± 3.5 Gyr (WMAP7), after which we obtain a rapid increase. The evolution of phantom potential is illustrated on Fig. 5.

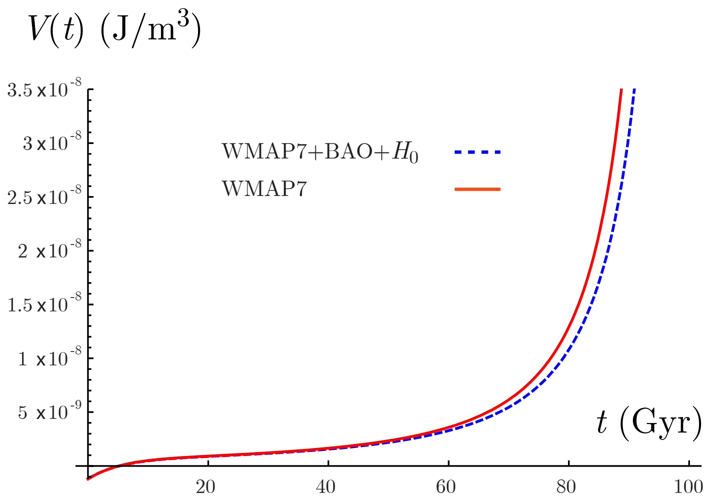

Figure 5. The phantom potential as function of t, obtained from observational data fitting of WMAP7 and WMAP7+BAO+H_0.

Now, concerning the scalar field evolution $\phi(t)$, at late times ($t \to t_{\rm s}$) the

ρ_{m0}-term in Eq. (4.13) can be neglected. Thus, Eq. (4.13) reduces to

$$\begin{aligned}\phi(t) &\approx \int\sqrt{\frac{2M_{\mathrm{P}}^2 c}{\hbar}\frac{|\beta|}{(t_{\mathrm{s}}-t)^2}}\,\mathrm{d}t \\ &= -\frac{2M_{\mathrm{P}}^2 c}{\hbar}|\beta|\ln(t_{\mathrm{s}}-t)\end{aligned} \tag{4.25}$$

which can be fitted using combined WMAP7+BAO+H_0 giving

$$\phi(t) \approx -2.64\times10^{13}\ln\left(3.30\times10^{18}-t\right), \tag{4.26}$$

while for WMAP7 dataset alone we obtain

$$\phi(t) \approx -2.63\times10^{13}\ln\left(3.23\times10^{18}-t\right). \tag{4.27}$$

As expected, both the phantom field and its kinetic energy $(-\dot{\phi}^2/2)$ diverge at the big rip.

Now we straightforwardly white the potential as a function of the phantom field, namely $V(\phi)$. In particular, Eq. (4.25) can be easily inverted, giving $t(\phi)$,

$$t(\phi) = t_{\mathrm{s}} - \mathrm{Exp}\left[-\frac{\hbar}{2\mathrm{M}_{\mathrm{P}}^2\mathrm{c}|\beta|}\phi\right]. \tag{4.28}$$

Thus substitution the equation above into Eq. (4.12) provides $V(\phi)$ at the late time as

$$V(\phi) = \frac{M_{\mathrm{P}}^2 c}{\hbar}\left(\frac{3|\beta|^2-|\beta|}{e^{-2\phi/\alpha}}\right) + \frac{|\beta|c^2(t_{\mathrm{s}}-t_0)^{-3|\beta|}}{2e^{3|\beta|\phi/\alpha}}, \tag{4.29}$$

where $\alpha \equiv (2M_{\mathrm{P}}^2 c|\beta|/\hbar)^{1/2}$. Doing so, for the combined data WMAP7+BAO+H_0 the potential is fitted as

$$V(\phi) \approx 6.47\times10^{27}\,e^{0.75\times10^{-13}\phi} - 2.51\times10^{-371}\,e^{-7.4\times10^{-13}\phi}, \tag{4.30}$$

while for WMAP7 dataset alone we obtain

$$V(\phi) \approx 6.37\times10^{27}\,e^{0.76\times10^{-13}\phi} - 1.99\times10^{-368}\,e^{-7.4\times10^{-13}\phi}. \tag{4.31}$$

In order to provide a more transparent picture, in Fig. 6 we present the corresponding plot for $V(\phi)$, for both the WMAP7+BAO+H_0 as well as the WMAP7 case.

Let us now consider the equation-of-state parameter for the phantom field, that is for the dark energy sector. As we mentioned in the end of section 4.1, it is

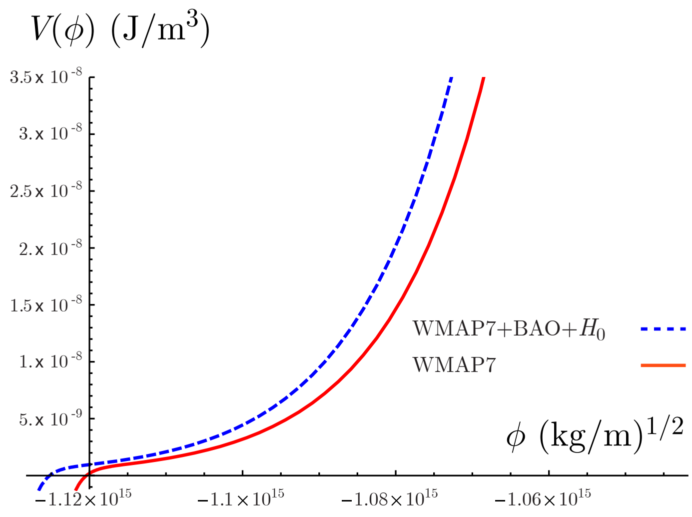

Figure 6. The phantom potential as function of ϕ, obtained from observational data fitting of WMAP7 and WMAP7+BAO+H_0.

given by $w_{\rm DE}(t) = p_\phi(t)/\rho_\phi(t)$, with $p_\phi(t)$ and $\rho_\phi(t)$ given by relations (4.15) and (4.14) respectively. We prefer to white $w_{\rm DE}$ as function of redshift z by using the relation Eq. (2.23),

$$1 + z = \frac{a_0}{a} = \left(\frac{t_{\rm s} - t_0}{t_{\rm s} - t}\right)^\beta . \tag{4.32}$$

By substitution equation above into Eq. (4.15) and (4.14). One can therefore use WMAP7 and WMAP7+BAO+H_0 observational data in order to fit the evolution of $w_{\rm DE}(z)$ at late times, that is for $t \to t_{\rm s}$, or equivalently for $z \to -1$. For the WMAP7+BAO+H_0 combined dataset we find

$$w_{\rm DE}(z) \approx \frac{1}{2} - \frac{6.068}{3.670 - (1+z)^{3.307}}, \tag{4.33}$$

while for the WMAP7 dataset alone we have

$$w_{\rm DE}(z) \approx \frac{1}{2} - \frac{6.328}{3.824 - (1+z)^{3.309}}. \tag{4.34}$$

As we observe, at $t \to t_{\rm s}$, $w_{\rm DE}$ becomes -1.153 for the combined dataset and -1.155 for the WMAP7 dataset alone. However, the phantom dark energy density and pressure become infinite. These behaviors are the definition of a big rip [44], and this acts as a self-consistency test of our model.

CHAPTER V

CONCLUSIONS

In this thesis we study dark energy models for explain accelerating expansion of the universe. We investigated phantom cosmology in which the scale factor is a power law. After constructing the scenario, we used observational data in order to impose constraints on the model parameters, focusing on the power-law exponent β and on the big rip time $t_{\rm s}$.

Using the WMAP7 dataset alone, we found that the power-law exponent is $\beta \approx -6.5 \pm 0.4$ while the big rip is realized at $t_{\rm s} \approx 102.3 \pm 3.5$ Gyr, in 1σ confidence level. Additionally, the dark-energy equation-of-state parameter $w_{\rm DE}$ lies always below the phantom divide as expected, and at the big rip it remains finite and equal to -1.155. However, both the phantom dark-energy density and pressure diverge at the big rip.

Using WMAP7+BAO+H_0 combined observational data we found that $\beta \approx -6.51^{+0.24}_{-0.25}$, while $t_{\rm s} \approx 104.5^{+1.9}_{-2.0}$ Gyr, in 1σ confidence level. Moreover, $w_{\rm DE}$ at the big rip becomes -1.153. Finally, in order to present a more transparent picture, we provided the reconstructed phantom potential.

In summary, we observe that phantom power-law cosmology can be compatible with observations, exhibiting additionally the usual phantom features, such is the future big rip singularity. However, it exhibits also the known disadvantage that the dark-energy equation-of-state parameter lies always below the phantom divide, by construction. In order to acquire a more realistic picture, describing also the phantom divide crossing, as it might be the case according to observations, one should proceed to the investigation of quintom power-law cosmology, considering apart from the phantom a canonical scalar field, too. Such a project is left for future investigation.

REFERENCES

REFERENCES

[1] Ahn, C., Kim, C. and Linder, E. V. (2009). Dark Energy Properties in DBI Theory. **Phys. Rev. D**, 80(12), 123016. [arXiv:0909.2637 [astro-ph.CO]].

[2] Amendola, L. and Tsujikawa, S. (2010). **Dark energy: theory and observations**, New York: Cambridge University Press.

[3] Armendariz-Picon, C., Mukhanov, V. F. and Steinhardt, P. J. (2000). A dynamical solution to the problem of a small cosmological constant and late-time cosmic acceleration. **Phys. Rev. Lett.**, 85(21), 4438-4441. [arXiv:astro-ph/0004134].

[4] Armendariz-Picon, C., Mukhanov, V. F. and Steinhardt, P. J. (2001). Essentials of k-essence. **Phys. Rev. D**, 63(10), 103510. [arXiv:astro-ph/0006373].

[5] Bagla, J. S., Jassal, H. K. and Padmanabhan, T. (2003). Cosmology with tachyon field as dark energy. **Phys. Rev. D**, 67(6), 063504. [arXiv:astro-ph/0212198].

[6] Bengochea, G. R. (2011). Supernova light-curve fitters and Dark Energy. **Phys. Lett. B**, 696(1-2), 5-12. [arXiv:1010.4014 [astro-ph.CO]].

[7] Caldwell, R. R. (2002). A Phantom Menace? Cosmological consequences of a dark energy component with super-negative equation of state. **Phys. Lett. B**, 545(1-2), 23-29. [arXiv:astro-ph/9908168].

[8] Caldwell, R. R., Dave, R., and Steinhardt, P. J. (1998). Cosmological Imprint of an Energy Component with General Equation-of-State, **Phys. Rev. Lett.**, 80(8), 1582-1585. [arXiv:astro-ph/9708069].

[9] Caldwell, R. R., Kamionkowski, M. and Weinberg, N. N. (2003). Phantom Energy: Dark Energy with $w < -1$ Causes a Cosmic Doomsday. **Phys. Rev. Lett.**, 91(7), 071301. [arXiv:astro-ph/0302506].

[10] Carretta, E., Gratton, R. G., Clementini, G., and Fusi Pecci, F. (2000). Distant, ages and epoch of formation of globular clusters. **Astrophys. J.**, 533(1), 215-235. [arXiv:astro-ph/9902086].

[11] Carroll, S. M. (1998). Quintessence and the rest of the world. **Phys. Rev. Lett.**, 81(15), 3067-3070. [arXiv:astro-ph/9806099].

[12] Carroll, S. M., Hoffman, M. and Trodden, M. (2003). Can the dark energy equation-of-state parameter w be less than -1? **Phys. Rev. D**, 68(2), 023509. [arXiv:astro-ph/0301273].

[13] Carroll, Sean M., Press, W. H. and Turner, E. L. (1992). The Cosmological Constant. **Annu. Rev. Astron. Astrophys.**, 30, 449-542.

[14] Chandrasekhar, S. (1931). The maximum mass of ideal white dwarfs. **Astrophys. J.**, 74, 81.

[15] Chiba, T., Okabe, T. and Yamaguchi, M. (2000). Kinetically driven quintessence. **Phys. Rev. D**, 62(2), 023511. [arXiv:astro-ph/9912463].

[16] Choudhury, T. R. and Padmanabhan, T. (2005). Cosmological parameters from supernova observations: A Critical comparison of three data sets. **Astron. Astrophys.**, 429(3), 807-818. [arXiv:astro-ph/0311622].

[17] Copeland, E. J., Sami, M. and Tsujikawa, S. (2006). Dynamics of dark energy. **Int. J. Mod. Phys. D**, 15(11), 1753-1935. [arXiv:hep-th/0603057].

[18] Das, S., Corasaniti, P. S. and Khoury, J. (2006). Super-acceleration as signature of dark sector interaction. **Phys. Rev. D**, 73(8), 083509. [arXiv:astro-ph/0510628].

[19] Guth, A. H. (1981). Inflationary universe: A possible solution to the horizon and flatness problems. **Phys. Rev. D**, 23(2), 347-356.

[20] Hansen, B. M. S. et al. (2002). The white dwarf cooling sequence of the globular custer Messier 4. **Astrophys. J.**, 574(2), L155-L158. [arXiv:astro-ph/0205087]

[21] Hicken, M., et al. (2009). Improved Dark Energy Constraints from 100 New CfA Supernova Type Ia Light Curves. **Astrophys. J.**, 700(2), 1097. [arXiv:0901.4804 [astro-ph.CO]].

[22] Hillebrandt, W. and Niemeyer, J. C. (2000). Type Ia supernova explosion models. **Ann. Rev. Astron. Astrophys.**, 38, 191-230. [arXiv:astro-ph/0006305].

[23] Hobson, M. P., Efstathiou, G. P. and Lasenby, A. N. (2006). **General relativity: an introduction for physicists**, New York: Cambridge University Press.

[24] Hubble, E. (1929). A Relation between Distance and Radial Velocity among Extra-Galactic Nebulae. **Proc. Nat. Acad. Sci.**, 15, 168-173.

[25] d'Inverno, R. (1996). **Introducing Einstein's relativity**, New York: Oxford University Press.

[26] Islam, Jamal N. (2002). **An introduction to mathematical cosmology**, Cambridge: Cambridge University Press.

[27] Jimenez, R., Thejll, P., Jorgensen, U., MacDonald, J., and Pagel, B. (1996). Ages of globular clusters: a new appoach. **Mon. Not. Roy. Astron. Soc.** 282(3), 926-942. [arXiv:astro-ph/9602132]

[28] Johri, V. B. (2004). Phantom cosmologies. **Phys. Rev. D**, 70(4), 041303. [arXiv:astro-ph/0311293].

[29] Kaeonikhom, C., Gumjudpai, B. and Saridakis, E. N. (2011). Observational constraints on phantom power-law cosmology. **Phys. Lett. B**, 695(1-4), 45-54. [arXiv:1008.2182 [astro-ph.CO]].

[30] Kaplinghat, M. and Rajaraman, A. (2007). Stable models of superacceleration. **Phys. Rev. D**, 75(10), 103504. [arXiv:astro-ph/0601517].

[31] Kessler, R., et al. (2009). First-year Sloan Digital Sky Survey-II (SDSS-II) Supernova Results: Hubble Diagram and Cosmological Parameters. **Astrophys. J. Suppl.**, 185(1), 32-84. [arXiv:0908.4274 [astro-ph.CO]].

[32] Komatsu, E., et al. [WMAP Collaboration]. (2009). Five-Year Wilkinson Microwave Anisotropy Probe (WMAP) Observations: Cosmological Interpretation. **Astrophys. J. Suppl.**, 180(2), 330. [arXiv:0803.0547 [astro-ph]].

[33] Komatsu, E., et al. [WMAP Collaboration]. (2011). Seven-Year Wilkinson Microwave Anisotropy Probe (WMAP) Observations: Cosmological Interpretation. **Astrophys. J. Suppl.** 192(2), 18. [arXiv:1001.4538 [astro-ph.CO]].

[34] Kowalski, M., et al. [Supernova Cosmology Project Collaboration]. Improved Cosmological Constraints from New, Old and Combined Supernova Datasets. **Astrophys. J.**, 686(2), 749. [arXiv:0804.4142 [astro-ph]].

[35] Larson, D. et al. (2011). Seven-Year Wilkinson Microwave Anisotropy Probe (WMAP) Observations: Power Spectra and WMAP-Derived Parameters. **Astrophys. J. Suppl.**, 192(2), 16. [arXiv:1001.4635 [astro-ph.CO]].

[36] Lemaître, G. (1931). **Expansion of the universe, A homogeneous universe of constant mass and increasing radius accounting for the radial velocity of extra-galactic nebulae**. (Eddington, A. S. and Lemaître, G., Trans.). London: Monthly Notices of the Royal Astronomical Society. (Original work published in Belgium 1927).

[37] Liddle, A. R. and Lyth, David H. (2000). **Cosmological inflation and large-scale structure**, Cambridge: Cambridge University Press.

[38] Liddle, A. (2003). **An introduction to modern cosmology**, Chichester: John Wiley & Sons Ltd.

[39] Lyons, L. (1991). **A practical guide to data analysis for physical science students**, Cambridge: Cambridge University Press.

[40] Martin, J. and Yamaguchi, M. DBI-essence. **Phys. Rev. D**, 77(12), 123508. [arXiv:0801.3375 [hep-th]].

[41] Mazzali, P. A., Ropke, F. K., Benetti, S. and Hillebrandt, W. (2007). A Common Explosion Mechanism for Type Ia Supernovae. **Science** 315(5813), 825-828. [arXiv:astro-ph/0702351].

[42] Nojiri, S. and Odintsov, S. D. (2006). Unifying phantom inflation with late-time acceleration: Scalar phantom-non-phantom transition model and generalized holographic dark energy. **Gen. Rel. Grav.**, 38(8), 1285-1304. [arXiv:hep-th/0506212].

[43] Nojiri, S., Odintsov, S. D. and Sasaki, M. (2005). Gauss-Bonnet dark energy. **Phys. Rev. D**, 71(12), 123509. [arXiv:hep-th/0504052].

[44] Nojiri, S., Odintsov, S. D. and Tsujikawa, S. (2005). Properties of singularities in (phantom) dark energy universe. **Phys. Rev. D**, 71(6), 063004. [arXiv:hep-th/0501025].

[45] Padmanabhan, T. and Choudhury, T. R. (2002). Can the clustered dark matter and the smooth dark energy arise from the same scalar field? **Phys. Rev. D**, 66(8), 081301. [arXiv:hep-th/0205055].

[46] Peebles, P. J. E. and Ratra, Bharat. (2003). The cosmological constant and dark energy. **Rev. Mod. Phys.**, 75(2), 559606.

[47] Percival, W. J., et al. (2010). Baryon Acoustic Oscillations in the Sloan Digital Sky Survey Data Release 7 Galaxy Sample. **Mon. Not. Roy. Astron. Soc.**, 401(4), 2148-2168. [arXiv:0907.1660 [astro-ph.CO]].

[48] Perlmutter, S., et al. (1999). [Supernova Cosmology Project Collaboration]. Measurements of Omega and Lambda from 42 High-Redshift Supernovae. **Astrophys. J.**, 517(2), 565. [arXiv:astro-ph/9812133].

[49] Riess, A. G., et al. (1998). Observational Evidence from Supernovae for an Accelerating Universe and a Cosmological Constant. **Astrophys. J.**, 116(3), 1009. [arXiv:astro-ph/9805201].

[50] Riess, A. G., et al. (2004). [Supernova Search Team Collaboration]. Type Ia supernova discoveries at $z > 1$ from the Hubble Space Telescope: Evidence for past deceleration and constraints on dark energy evolution. **Astrophys. J.**, 607(2), 665. [arXiv:astro-ph/0402512].

[51] Riess, A. G., et al. (2009). A Redetermination of the Hubble Constant with the Hubble Space Telescope from a Differential Distance Ladder," **Astrophys. J.**, 699(1), 539. [arXiv:0905.0695 [astro-ph.CO]].

[52] Singh, P., Sami, M. and Dadhich, N. (2003). Cosmological dynamics of phantom field. **Phys. Rev. D**, 68(2), 023522. [arXiv:hep-th/0305110].

[53] Starobinsky, A. A. (2000). Future and origin of our universe: Modern view. **Grav. Cosmol.**, 6, 157-163. [arXiv:astro-ph/9912054].

[54] Stern, D., Jimenez, R., Verde, L., Kamionkowski, M. and Stanford, S. A. (2010). Cosmic chronometers: constraining the equation of state of dark energy. I: $H(z)$ measurements. **JCAP**, 2010(02), 008. [arXiv:0907.3149 [astro-ph.CO]].

[55] Weinberg, S. (1989). The Cosmological Constant Problem. **Rev. Mod. Phys.**, 61(1), 123.

[56] Weinberg, S. (October 7, 1996). **Theories of the cosmological constant**. Retrived November 2, 2010 from http://arxiv.org/abs/astro-ph/9610044 [arXiv:astro-ph/9610044].

[57] Yoon, S. C. and Langer, N. (2004). Presupernova evolution of accreting white dwarfs with rotation. **Astron. Astrophys.**, 419(2), 623-644. [arXiv:astro-ph/0402287].

[58] Zlatev, I., Wang, L. M., and Steinhardt, P. J. (1999). Quintessence, Cosmic Coincidence, and the Cosmological Constant. **Phys. Rev. Lett.**, 82(5), 896. [arXiv:astro-ph/9807002].

APPENDICES

APPENDIX A NOTES OF THIS THESIS

In the Table 3, estimation the time at big rip t_{s} via Eq. (4.22), I have used $w_{\mathrm{DE}} = -1.12$ [35] from WMAP7 alone, while other using parameters are taken from WMAP7+BAO+H_0 dataset. However, the true value of these parameters from WMAP7 +BAO+H_0 are shown in the new table, as follows

Parameter	**WMAP7+BAO+H_0**	**WMAP7**
β	$-7.82^{+0.22}_{-0.23}$	-6.5 ± 0.4
ρ_{m0}	$(2.52 \pm 0.26) \times 10^{-27}$ kg/m^3	$(2.50 \pm 0.30) \times 10^{-27}$ kg/m^3
ρ_{c0}	$(9.3^{+0.3}_{-0.4}) \times 10^{-27}$ kg/m^3	$(9.57 \pm 0.67) \times 10^{-27}$ kg/m^3
t_{s}	$122.7^{+2.3}_{-2.4}$ Gyr	102.3 ± 3.5 Gyr
	[$(3.87^{+0.07}_{-0.08}) \times 10^{18}$ sec]	[$(3.23 \pm 0.11) \times 10^{18}$ sec].

Table 4. The table shows the true parameter values, which using $w_{\mathrm{DE}} = -1.10$ [33] from WMAP+BAO+H_0. The changed values from Table 3 are power-law exponent and the big rip time, while other parameters remain the same.

Moreover, the phantom potential in Eq. (4.23) is changed to the true value namely

$$V(t) \approx \frac{9.40 \times 10^{27}}{(3.87 \times 10^{18} - t)^2} - 2.59 \times 10^{-445}(3.87 \times 10^{18} - t)^{23.45}, \tag{A.1}$$

which the true inflection happen at 24.06 Gyr. Comparing with WMAP7 dataset alone is shown in Fig. 7. We see that the phantom potential using $w_{\mathrm{DE}} = -1.10$ is slower increase than WMAP7 dataset alone. A little deviation of w_{DE} immensely influences deviation of other variables.

The scalar field evolution at the late time of true WMAP7 combined dataset are fitted as

$$\phi(t) \approx -2.89 \times 10^{13} \ln (3.87 \times 10^{18} - t), \tag{A.2}$$

and it can easily inverted as

$$V(\phi) \approx 9.40 \times 10^{27}\, e^{6.91\times 10^{-14}\phi} - 2.59 \times 10^{-445}\, e^{-8.1\times 10^{-13}\phi}. \tag{A.3}$$

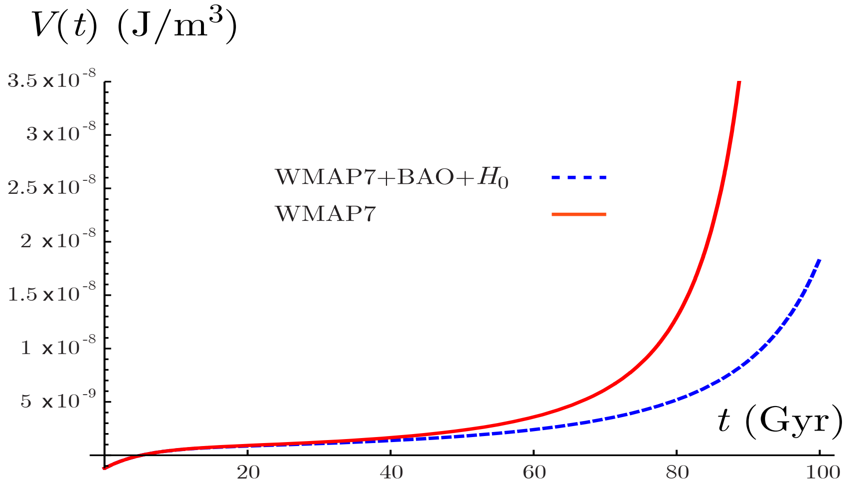

Figure 7. The phantom potential of the true value for WMAP7+BAO+H_0 dataset and WMAP7 dataset alone

The true field potential $V(\phi)$ from combined data remains consistent with phantom scenario. A different thing to WMAP7 dataset alone is that $V(\phi)$ of combined data is more rapidly increased when ϕ in creases than $V(\phi)$ from WMAP7 dataset alone. This $V(\phi)$ from two datasets may not be implicitly illustrated in the same range. We then chose not to show plotting for comparison of two datasets.

The equation-of-state parameter at the late time estimating from true WMAP7 combined dataset approaches to $w_{\rm DE} \approx -1.128$, which has a small deviate from the present value.

Indeed, the equation-of-state parameter of phantom dark energy is very sensitive to the value of the time at big rip $t_{\rm s}$. In details, we consider plotting of $t_{\rm s}$ versus $w_{\rm DE}$, which given by equation

$$t_{\rm s} \simeq t_0 + \frac{2}{3}|1 + w_{\rm DE}|^{-1} H_0^{-1}(1 - \Omega_{\rm m0})^{-1/2}. \tag{A.4}$$

Plotting of $t_{\rm s}$ versus $w_{\rm DE}$ as shown in Fig. 8 shows small variation of $w_{\rm DE}$ can dramatic changes the value of $t_{\rm s}$. There is a good way to exclude error bar from $w_{\rm DE}$ for estimating $t_{\rm s}$

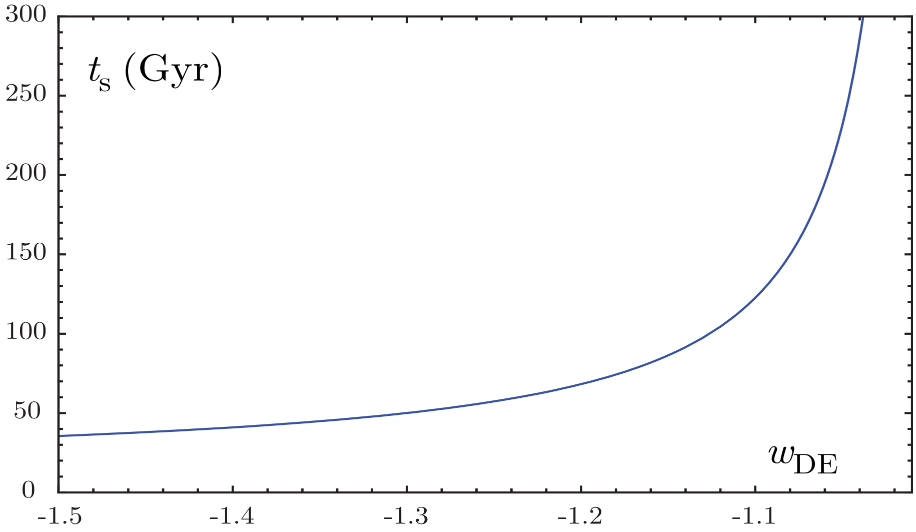

Figure 8. Plotting of big rip time t_s versus equation-of-state parameter of dark energy w_{DE}

w_{DE}	t_s (Gyr)	w_{DE}	t_s (Gyr)
-1.06	195.25	-1.16	81.83
-1.08	149.88	-1.18	74.27
-1.10	122.66	-1.20	68.22
-1.12	104.51	-1.22	63.27
-1.14	91.55	-1.24	59.15

Table 5. Relation between the value of dark energy equation-of-state parameter w_{DE} and the value of big rip time t_s

APPENDIX B ESTIMATION FOR ERROR

We are frequently confronted with observational data, which giving in many terms of measurements. Then we need to know what is the error on the final answer, which are given by individual measurements. We conclude that, for general case, an answer f of n measured quantities can be obtained via the method as follows, defining

$$f = f(x_1, x_2, ..., x_i, ..., x_n), \tag{B.1}$$

where x_i are the measured quantities . Differentiation of f gives

$$\delta f = \frac{\partial f}{\partial x_1}\delta x_1 + \frac{\partial f}{\partial x_2}\delta x_2 + ... + \frac{\partial f}{\partial x_n}\delta x_n. \tag{B.2}$$

Squaring and averaging over a whole terms of measurement, which all the cross terms like $\delta x_1 \delta x_2$, vanished [4] then we find

$$(\delta f)^2 = \sum_{i=1}^{n} \left(\frac{\partial f}{\partial x_i}\right)^2 (\delta x_i)^2. \tag{B.3}$$

The quantities δf and δx_i are indeed the errors of f and measured quantities x_i, then we change notation as $\delta f \to \sigma_f$ and $\delta x_i \to \sigma_i$, we finally obtain

$$\sigma_f^2 = \sum_{i=1}^{n} \left(\frac{\partial f}{\partial x_i}\right)^2 \sigma_i^2. \tag{B.4}$$

Note that Eq. (B.4) is usually used for small error. For example, estimating error of $t_{\rm s}$ (WMAP7 dataset alone), we start from considering

$$t_{\rm s} = t_0 + \frac{2}{3}|1 + w_{\rm DE}|^{-1} H_0^{-1} (1 - \Omega_{\rm m0})^{-1/2}. \tag{B.5}$$

Therefore the error of $t_{\rm s}$ can be found from

$$\sigma_{t_{\rm s}}^2 = \left(\frac{\partial t_{\rm s}}{\partial t_0}\right)^2 \sigma_{t_0}^2 + \left(\frac{\partial t_{\rm s}}{\partial H_0}\right)^2 \sigma_{H_0}^2 + \left(\frac{\partial t_{\rm s}}{\partial \Omega_{\rm m0}}\right)^2 \sigma_{\Omega_{\rm m0}}^2. \tag{B.6}$$

---

[4] If different x_i are uncorrelated, then all of cross terms vanish. See also in Section 1.7 of reference [39]

We have

$$\begin{aligned}
\frac{\partial t_{\rm s}}{\partial t_0} &= 1, \\
\frac{\partial t_{\rm s}}{\partial H_0} &= \frac{2}{3H_0^2(1+w_{\rm DE})(1-\Omega_{\rm m0})^{1/2}}, \\
\frac{\partial t_{\rm s}}{\partial \Omega_{\rm m0}} &= -\frac{2}{3H_0(1+w_{\rm DE})(1-\Omega_{\rm m0})^{3/2}},
\end{aligned} \tag{B.7}$$

then substituting these observed quantities as shown on the right column of Table 2, we find $t_{\rm s} = 102.3 \pm 3.5$ billion years (see Mathematica code in Appendix C).

APPENDIX C MATHEMATICA CODE

C.1 Code for plotting in Fig. 1

```
In[1]:= (* Changing unit *)
gyr = 3.15576 10^16;      (* 1 Gigayear *)
hunit = 10^(-19)/3.086;   (* Hubble constant in SI unit *)
hzero = 70.2 hunit;       (* maximum likelihood value of WMAP7 data *)
(* ------------------------ *)
In[4]:= (* flat with DE *)
t0DE[Omgm_]:= 1/(3 Sqrt[1-Omgm])Log[(1 + Sqrt[1-Omgm])/(1
-Sqrt[1-Omgm])];
(* open without DE *)
t0k[Omgm_]:= 1/(1-Omgm)(1+Omgm/(2 Sqrt[1-Omgm])Log[(1-Sqrt[1-Omgm])/(1
+Sqrt[1-Omgm])]);
Glob := 11 gyr hzero;
(* WMAP 7-year bound *)
WMAPbndUp := 13.89 gyr hzero;
WMAPbndLo := 13.67 gyr hzero;

Plot[{t0DE[Omgm], t0k[Omgm], WMAPbndUp, WMAPbndLo, Glob}, {Omgm, 0, 1},
PlotRange -> {{0, 1}, {0.6, 1.6}}, Axes -> False, Frame -> True,
PlotStyle -> {{Blue, Thick}, {Red, Dashed}, Purple, Purple, LightGray},
Filling -> {{3 -> {{4}, LightRed}}, {5 -> {Axis, LightGray}}}]
Out[9]=
```

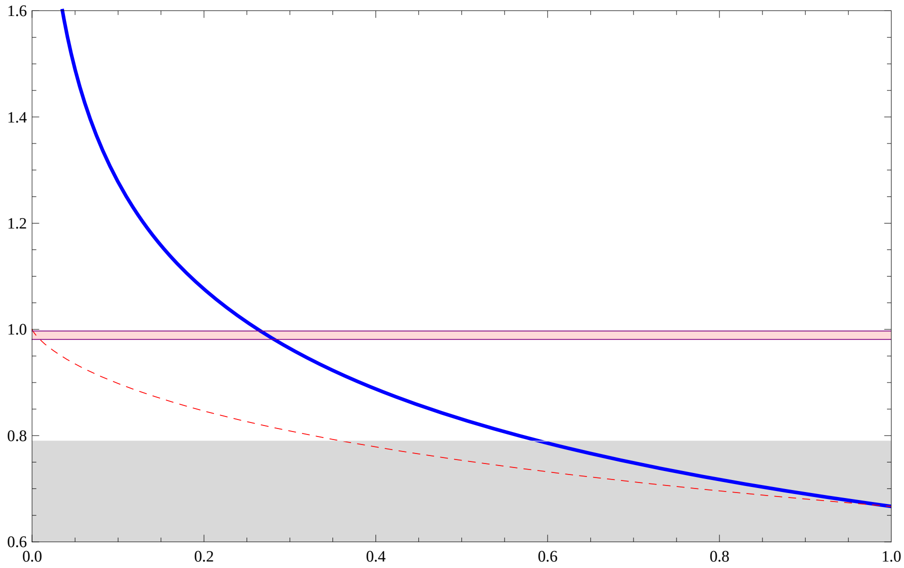


```
In[10]:= (* obtaining Omega_m *)

(* Lower bound *)

FindRoot[1/(3 Sqrt[1-Omgm])Log[(1+Sqrt[1-Omgm])/(1-Sqrt[1-Omgm])]

== 13.89 gyr hzero, {Omgm, 0.3}]

(* Upper bound *)

FindRoot[1/(3 Sqrt[1-Omgm])Log[(1+Sqrt[1-Omgm])/(1-Sqrt[1-Omgm])]

== 13.67 gyr hzero, {Omgm, 0.3}]


Out[10]= {Omgm -> 0.265656}

Out[11]= {Omgm -> 0.281499}


(* ==================== End of Code =================== *)
```

C.2 Code for plotting evolution of scale factor Fig. 2

```
In[1]:= (* density parameters for dust (Omgm) DE (OmgL) *)

Omgm1 = 0.3;

Omgm2 = 1;

OmgL1 = 0.7;
```

```
OmgL2 = 0;

OmgL3 = 1;

Omgk = 0.0085;

(* ---------------------------------- *)

In[7]:=

c = 2.99792458*10^8;   (* speed of light *)

(* ====================== *)

(* changing unit *)

gyr = 3.15576 10^16;

hunit = 10^(-19)/3.086;

H0 = 70.2 hunit;

Htdust = 2/(3 Sqrt[Omgm2]);  (* age of a universe--dust model *)

Htdust30 = 2/(3 Sqrt[Omgm1]);


In[13]:= (* age of a universe--LCDM *)

H0t0 = 1/(3 Sqrt[1 - Omgm1])Log[(1+Sqrt[1-Omgm1])/(1-Sqrt[1-Omgm1])];


In[14]:= aHt = Table[{N[Integrate[1/Sqrt[Omgm1 a^(-1)+OmgL1 a^2],

{a, 0, 0.05 i}]]-H0t0, 0.05 i}, {i, 0, 80}]


Out[14]= {{-0.950492,0.05},{-0.925624,0.1},{-0.893481,0.15},

{-0.855569,0.2},{-0.812864,0.25},{-0.766142,0.3},{-0.716094,0.35},

{-0.66337,0.4},{-0.608589,0.45},{-0.55234,0.5},{-0.495171,0.55},

{-0.437576,0.6},{-0.379988,0.65},{-0.322773,0.7},{-0.266232,0.75},

{-0.210599,0.8},{-0.156052,0.85},{-0.102719,0.9},{-0.0506847,0.95},

{-1.*10^-9,1.},{0.0493114,1.05},{0.0972471,1.1},{0.143821,1.15},

{0.189057,1.2},{0.232991,1.25},{0.27566,1.3},{0.317108,1.35},

{0.35738,1.4},{0.396522,1.45},{0.434578,1.5},{0.471595,1.55},

{0.507617,1.6},{0.542685,1.65},{0.576842,1.7},{0.610126,1.75},
```

```
{0.642576,1.8},{0.674226,1.85},{0.705112,1.9},{0.735266,1.95},
{0.764718,2.},{0.793498,2.05},{0.821632,2.1},{0.849149,2.15},
{0.876071,2.2},{0.902424,2.25},{0.928228,2.3},{0.953505,2.35},
{0.978275,2.4},{1.00256,2.45},{1.02637,2.5},{1.04973,2.55},
{1.07265,2.6},{1.09516,2.65},{1.11725,2.7},{1.13895,2.75},
{1.16028,2.8},{1.18123,2.85},{1.20184,2.9},{1.22209,2.95},
{1.24202,3.},{1.26163,3.05},{1.28092,3.1},{1.29991,3.15},
{1.31861,3.2},{1.33702,3.25},{1.35516,3.3},{1.37303,3.35},
{1.39064,3.4},{1.408,3.45},{1.42511,3.5},{1.44198,3.55},
{1.45862,3.6},{1.47503,3.65},{1.49122,3.7},{1.5072,3.75},
{1.52297,3.8},{1.53853,3.85},{1.5539,3.9},{1.56907,3.95},
{1.58405,4.}}

In[15]:= scalef=Interpolation[aHt]
Out[15]= InterpolatingFunction[{{-0.950492,1.58405}},<>]

In[16]:= (* evolution of a(t)--dust model *)
age2[t_]:= (3/2(t+Htdust))^(2/3);

In[17]:= Plot[{scalef[t], age2[t]},{t, -1.2, 2},PlotRange->{{-1.2, 2},
{0,4}}, Frame->True, Axes->False,AspectRatio->5/6,
PlotStyle->{{Red,Thick}, {Darker[Blue], Thick,Dashed}, {Blue}}]
Out[17]=
```

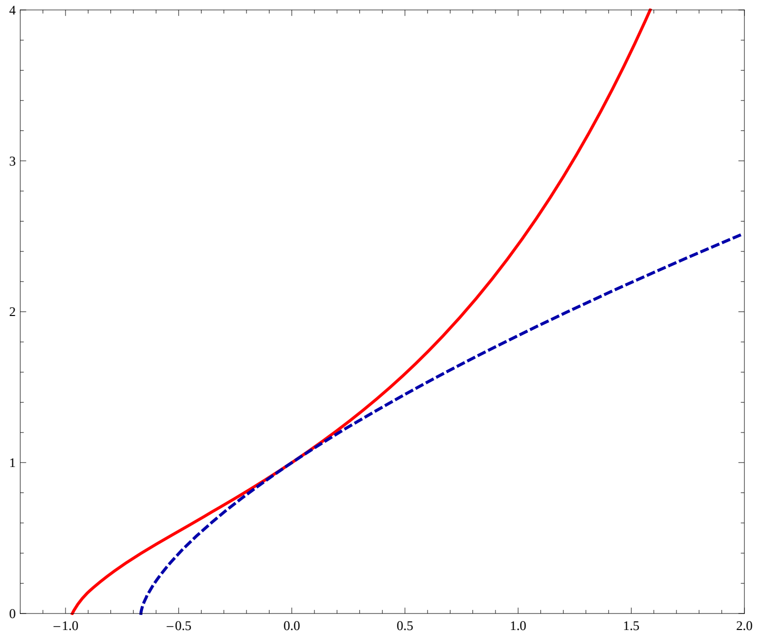

C.3 Code for plotting luminosity distance with SN Ia data Fig. 3

```
In[1]:= (* Omega_DE *)

OmgL1=0.7;

OmgL2=0;

OmgL3=1;


In[4]:= Ar1 = Table[{0.1i, Abs[N[(1+0.1i)Integrate[1/Sqrt[(1-OmgL1)
(1+z)^3+OmgL1], {z,0, 0.1i}]]]},{i,15}]


Out[4]= {{0.1,0.107478},{0.2,0.228841},{0.3,0.362551},{0.4,0.507189},
{0.5,0.661477},{0.6,0.824282},{0.7,0.994618},{0.8,1.17163},
{0.9,1.35459},{1.,1.54285},{1.1,1.73589},{1.2,1.93323},{1.3,2.13448},
{1.4,2.33928},{1.5,2.54734}}


In[5]:= dL1 = Interpolation[Ar1]

Out[5]= InterpolatingFunction[{{0.1,1.5}},<>]
```

```
In[6]:= dL3[x_]:= 2(1+x)-2Sqrt[1+x];   (* flat , OmgL = 0 *)
dL4[x_]:= (1+x)x/Sqrt[OmgL3] ; (* flat OmgL = 1 *)

In[8]:= dLPlot = Plot[{dL1[x], dL3[x], dL4[x]}, {x,0,2}, Frame->True,
Axes->False, PlotRange->{{0, 2}, {0, 4}}, AspectRatio->1,
PlotStyle->{{Darker[Green], Thick}, {Magenta, Thick, DotDashed},
{Red,Thick,Dashed}}];

(* ============================================================== *)
(* Speed of Light *)
c = 2.99792458*10^8;
(* ====================== *)
(* changing unit *)
gyr = 3.15576 10^16;
hunit = 10^(-19)/3.086;
H0 = 70.2 hunit;

In[13]:= (* Test for "Gold" SN Ia data from Reiss 2003
--using only observed data from the year 1997-2003 *)
m[1] = 42.57;       (* SN 1997aw *)
m[2] = 41.64;       (* SN 1997as *)
m[3] = 42.10;       (* SN 1997am *)
m[4] = 43.85;       (* SN 1997ap *)
m[5] = 42.86;       (* SN 1997af *)
m[6] = 41.76;       (* SN 1997bh *)
m[7] = 42.83;       (* SN 1997bb *)
m[8] = 40.92;       (* SN 1997bj *)
m[9] = 42.74;       (* SN 1997cj *)
m[10] = 42.08;      (* SN 1997ce *)
```

```
m[11] = 43.81;      (* SN 1997ez *)
m[12] = 44.03;      (* SN 1997ek *)
m[13] = 42.66;      (* SN 1997eq *)
m[14] = 45.53;      (* SN 1997ff *)
m[15] = 42.91;      (* SN 1998I *)
m[16] = 43.61;      (* SN 1998J *)
m[17] = 42.62;      (* SN 1998M *)
m[18] = 41.83;      (* SN 1998ac *)
m[19] = 43.35;      (* SN 1998bi *)
m[20] = 42.36;      (* SN 1998ba *)
m[21] = 42.56;      (* SN 1999Q *)
m[22] = 42.75;      (* SN 1999U *)
m[23] = 41.00;      (* SN 1999fw *)
m[24] = 44.25;      (* SN 1999fk *)
m[25] = 43.99;      (* SN 1999fm *)
m[26] = 43.76;      (* SN 1999fj *)
m[27] = 42.29;      (* SN 1999ff *)
m[28] = 44.19;      (* SN 1999fv *)
m[29] = 42.38;      (* SN 1999fn *)
m[30] = 42.75;      (* SN 2000dz *)
m[31] = 42.41;      (* SN 2000eh *)
m[32] = 42.74;      (* SN 2000ee *)
m[33] = 41.96;      (* SN 2000eg *)
m[34] = 42.77;      (* SN 2000ec *)
m[35] = 42.68;      (* SN 2000fr *)
m[36] = 43.75;      (* SN 2001fs *)
m[37] = 43.12;      (* SN 2001fo *)
m[38] = 43.97;      (* SN 2001hy *)
m[39] = 43.88;      (* SN 2001hx *)
```

```
m[40] = 43.55;      (* SN 2001hs *)
m[41] = 43.90;      (* SN 2001hu *)
m[42] = 40.71;      (* SN 2001iw *)
m[43] = 40.89;      (* SN 2001iv *)
m[44] = 42.88;      (* SN 2001iy *)
m[45] = 43.05;      (* SN 2001ix *)
m[46] = 42.77;      (* SN 2001jp *)
m[47] = 44.23;      (* SN 2001jh *)
m[48] = 44.09;      (* SN 2001jf *)
m[49] = 43.91;      (* SN 2001jm *)
m[50] = 42.14;      (* SN 2002dc *)
m[51] = 44.06;      (* SN 2002dd *)
m[52] = 45.27;      (* SN 2002fw *)
m[53] = 43.01;      (* SN 2002hr *)
m[54] = 44.70;      (* SN 2002hp *)
m[55] = 43.09;      (* SN 2002kd *)
m[56] = 44.84;      (* SN 2002ki *)
m[57] = 45.20;      (* SN 2003az *)
m[58] = 45.30;      (* SN 2003ak *)
m[59] = 43.19;      (* SN 2003bd *)
m[60] = 43.07;      (* SN 2003be *)
m[61] = 45.05;      (* SN 2003dy *)
m[62] = 44.28;      (* SN 2003es *)
m[63] = 43.86;      (* SN 2003eq *)
m[64] = 43.64;      (* SN 2003eb *)
m[65] = 43.87;      (* SN 2003lv *)
(* the last 10 data are obtained  before the whole 65 data *)
m[66] = 43.04;      (* SN 1997F *)
m[67] = 42.56;      (* SN 1997H *)
```

```
m[68] = 39.79;      (* SN 1997I *)
m[69] = 39.98;      (* SN 1997N *)
m[70] = 42.46;      (* SN 1997P *)
m[71] = 41.99;      (* SN 1997Q *)
m[72] = 43.27;      (* SN 1997R *)
m[73] = 42.10;      (* SN 1997ai *)
m[74] = 41.45;      (* SN 1997ac *)
m[75] = 42.63;      (* SN 1997aj *)
(*-------------------------------------------------------*)
(* redshift *)
z[1]=0.440;z[2]=0.508;z[3]=0.416;z[4]=0.830;z[5]=0.579;z[6]=0.420;
z[7]=0.518;z[8]=0.334;z[9]=0.500;z[10]=0.440;z[11]=0.778;z[12]=0.860;
z[13]=0.538;z[14]=1.755;z[15]=0.886;z[16]=0.828;z[17]=0.630;
z[18]=0.460;z[19]=0.740;z[20]=0.430;z[21]=0.460;z[22]=0.500;
z[23]=0.278;z[24]=1.056;z[25]=0.949;z[26]=0.815;z[27]=0.455;
z[28]=1.19;z[29]=0.477;z[30]=0.500;z[31]=0.490;z[32]=0.470;
z[33]=0.540;z[34]=0.470;z[35]=0.543;z[36]=0.873;z[37]=0.771;
z[38]=0.811;z[39]=0.798;z[40]=0.832;z[41]=0.882;z[42]=0.340;
z[43]=0.397;z[44]=0.570;z[45]=0.710;z[46]=0.528;z[47]=0.884;
z[48]=0.815;z[49]=0.977;z[50]=0.475;z[51]=0.95;z[52]=1.30;
z[53]=0.526;z[54]=1.305;z[55]=0.735;z[56]=1.140;z[57]=1.265;
z[58]=1.551;z[59]=0.67;z[60]=0.64;z[61]=1.340;z[62]=0.954;
z[63]=0.839;z[64]=0.899;z[65]=0.94;

(* the last 10 data are obtained  before the whole 65 data *)

z[66]=0.580;z[67]=0.526;z[68]=0.172;z[69]=0.180;z[70]=0.472;
z[71]=0.430;z[72]=0.657;z[73]=0.450;z[74]=0.320;z[75]=0.581;
```

```
(*-----------------------------------------------------------*)
(* Errors of relative magnitude *)
err[1]=0.40;err[2]=0.35;err[3]=0.19;err[4]=0.19;err[5]=0.19;
err[6]=0.23;err[7]=0.30;err[8]=0.30;err[9]=0.20;err[10]=0.19;
err[11]=0.35;err[12]=0.30;err[13]=0.18;err[14]=0.35;err[15]=0.81;
err[16]=0.61;err[17]=0.24;err[18]=0.40;err[19]=0.30;err[20]=0.25;
err[21]=0.27;err[22]=0.19;err[23]=0.41;err[24]=0.23;err[25]=0.25;
err[26]=0.33;err[27]=0.28;err[28]=0.34;err[29]=0.21;err[30]=0.24;
err[31]=0.25;err[32]=0.23;err[33]=0.41;err[34]=0.21;err[35]=0.19;
err[36]=0.38;err[37]=0.17;err[38]=0.35;err[39]=0.31;err[40]=0.29;
err[41]=0.30;err[42]=0.27;err[43]=0.30;err[44]=0.31;err[45]=0.32;
err[46]=0.25;err[47]=0.19;err[48]=0.28;err[49]=0.26;err[50]=0.19;
err[51]=0.26;err[52]=0.19;err[53]=0.27;err[54]=0.22;err[55]=0.19;
err[56]=0.30;err[57]=0.20;err[58]=0.22;err[59]=0.28;err[60]=0.21;
err[61]=0.25;err[62]=0.31;err[63]=0.22;err[64]=0.25;err[65]=0.20;

(* the last 10 data are obtained  before the whole 65 data *)

err[66]=0.21;err[67]=0.18;err[68]=0.18;err[69]=0.18;err[70]=0.19;
err[71]=0.18;err[72]=0.20;err[73]=0.23;err[74]=0.18;err[75]=0.19;

(*-----------------------------------------------------------*)
DL[m_]:=H(P)10^(m/5)/v;
DL'[m]
Table[{z[j],H0(3.086 * 10^17)10^(m[j]/5)/c},{j,75}];
Table[{err[k]},{k,75}];

In[242]:= Table["ErrorBar"[err[l]],{l,75}];
ErrTable = Table[{{z[j],H0(3.086 * 10^17)10^(m[j]/5)/c},
```

```
ErrorBar[H0 (3.086 * 10^17)2^(m[j]/5)5^(-1+m[j]/5)err[j]/c]},{j,75}];

In[244]:= Needs["ErrorBarPlots`"]
errPlot=ErrorListPlot[Table[{{z[j],H0(3.086 * 10^17)
10^(m[j]/5)/c},ErrorBar[H0 (3.086 * 10^17)2^(m[j]/5)5^(-1+m[j]/5)
err[j]/c]},{j,75}], AxesOrigin->{0,0},PlotStyle->{Black}] ;
LogerrPlot=ErrorListPlot[Table[{{z[j],Log[10,H0(3.086 * 10^17)
10^(m[j]/5)/c]},ErrorBar[Log[10,H0(3.086 * 10^17)10^(m[j]/5)/c+H0
(3.086 * 10^17)2^(m[j]/5)5^(-1+m[j]/5)err[j]/c]-Log[10,H0(3.086
* 10^17)10^(m[j]/5)/c]]},{j,75}],AxesOrigin->{0,0},
PlotStyle->{Black}] ;

In[247]:= Show[dLPlot, errPlot]
Out[247]=
```

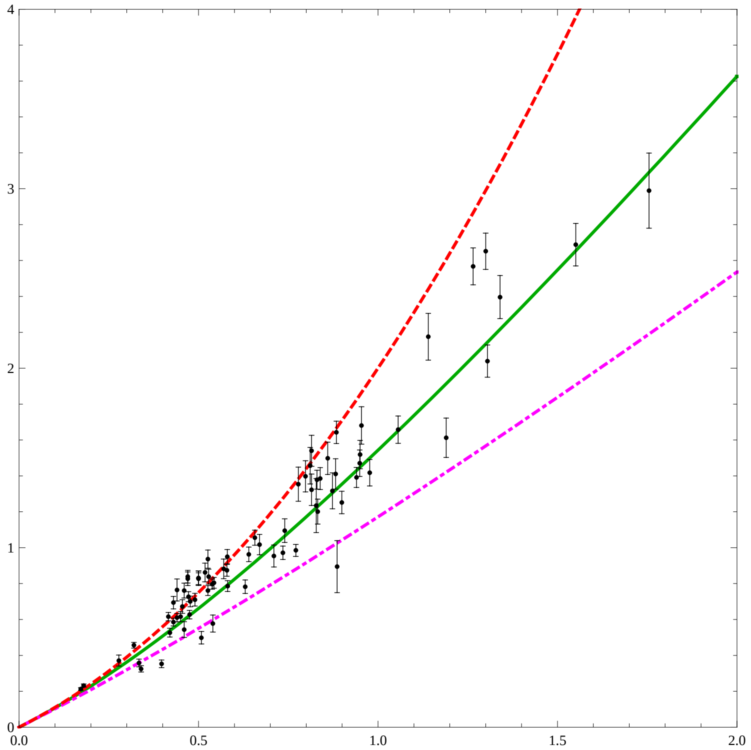

C.4 Code for secondary fitted parameters in Chapter 4

```
In[172]:= (* Fundamental constants *)
c = 2.99792458*10^8;         (* The speed of light *)
g = 6.674*10^-11;            (* Gravitational constant *)
hbar = 1.055*10^-34;         (* Planck's constant *)
(* =================== *)
mp = Sqrt[(hbar*c)/(8Pi*g)]; (* Reduced Planck mass *)
(* ====================== *)

(* changing unit *)
gyr = 3.15576 10^16;         (* Gigayear -> second *)
hunit = 10^(-19)/3.086;      (* Hubble parameter in [time]^{-1} unit *)
(* ============================================================== *)

(* Observational parameter *)
(* 1 for WMAP7+BAO+H0, 2 for WMAP7 alone *)

hzero1 = 70.2 hunit;             (* Hubble parameter *)
hzero2 = 71.4 hunit;
omegab1 = 0.0455;                (* baryonic density parameter*)
omegab2 = 0.0445;
omegac1 = 0.227;                 (* cold dark mater density parameter*)
omegac2 = 0.217;
omegadust1 := omegab1+omegac1;   (* cold dark mater density parameter*)
omegadust2 := omegab2+omegac2;
tzero1 := 13.78 gyr;             (* the present time *)
tzero2 := 13.71 gyr;
w = -1.12;                       (* Equation-of-state parameter *)
(* ============================================================== *)
(* The Big Rip time *)
```

```
trip1 = tzero1-(2/3 ) 1/(1+w)*hzero1^-1*(1-omegadust1)^(-1/2);
trip2 = tzero2-(2/3 ) 1/(1+w)*hzero2^-1*(1-omegadust2)^(-1/2);
tripgyrunit1= trip1/gyr;(* The Big Rip time in unit of billion years *)
tripgyrunit2= trip2/gyr;

rhoc1 = (3 hzero1^2)/(8 Pi g);          (* Critical density *)
rhoc2 = (3 hzero2^2)/(8 Pi g);
rhom1 =  omegadust1 rhoc1;              (* Matter density *)
rhom2 =  omegadust2 rhoc2;
q1 = -hzero1 (trip1-tzero1) ;           (* Power-law exponent *)
q2 = -hzero2 (trip2-tzero2) ;
d1 = omegadust1 rhoc1;                  (* Density constant *)
d2 = omegadust2 rhoc2;
alpha1= Sqrt[(-2mp^2c q1)/hbar];        (* definition for simplicity *)
alpha2= Sqrt[(-2mp^2c q2)/hbar];

In[203]:= (* For WMAP7+BAO+H0 dataset *)
d1
tzero1
q1
rhom1
rhoc1
tripgyrunit1
(* ---------------------------------- *)
Out[203]= 2.52199*10^-27
Out[204]= 4.34864*10^17
Out[205]= -6.51345
Out[206]= 2.52199*10^-27
Out[207]= 9.25502*10^-27
```

```
Out[208]= 104.513
(* ================================================================ *)
In[209]:=   (* For WMAP7 dataset alone *)
d2
tzero2
q2
rhom2
rhoc2
tripgyrunit2
(* ----------------------------------- *)
Out[209]= 2.50364*10^-27
Out[210]= 4.32655*10^17
Out[211]= -6.46476
Out[212]= 2.50364*10^-27
Out[213]= 9.57414*10^-27
Out[214]= 102.251
(* ================================================================ *)

In[215]:= (* phantom potential *)
V1[t_]:=(mp^2 c)/hbar *((3 q1^2+q1)/(trip1-t)^2)
- d1 c^2 (trip1-tzero1)^(3 q1)/(2(trip1-t)^(3 q1));

V2[t_]:=(mp^2 c)/hbar *((3 q2^2+q2)/(trip2-t)^2)
- d2 c^2 (trip2-tzero2)^(3 q2)/(2(trip2-t)^(3 q2));

V1[t]
V2[t]

Out[217]= 6.47059*10^27/(3.29818*10^18-t)^2
```

```
-2.516125664325231*10^-371 (3.29818*10^18-t)^19.5403

Out[218]= 6.37163*10^27/(3.22681*10^18-t)^2
-1.993330768839323*10^-368 (3.22681*10^18-t)^19.3943
(* ----------------------------------------------------------------- *)

In[219]:= (* The time at inflection *)
FindRoot[V1'[tinflect1] == 0,{tinflect1,3*10^18}]
(tinflect1/.%)/gyr
Out[219]= {tinflect1->7.08056*10^17}
Out[220]= 22.4369

In[221]:= FindRoot[V2'[tinflect2] == 0,{tinflect2,3*10^18}]
(tinflect2/.%)/gyr
Out[221]= {tinflect2->6.94329*10^17}
Out[222]= 22.002

(* ========================= Plot V(t) =============================*)
In[233]:= (* Blue-dashed for WMAP7+BAO+H0 dataset, Red-thick for WMAP7
dataset alone *)
V1Plot :=
  Plot[V1[t], {t, 0, 100 gyr}, PlotRange -> {V1[0], 3.5 10^(-8)},
   Ticks -> {{{6.31152 10^17, "20"}, {1.2623 10^18,
       "40"}, {1.89346 10^18, "60"}, {2.52461 10^18,
       "80"}, {3.15576 10^18, "100"}}, Automatic},
   PlotStyle -> {Thick, Dashed, Blue}];
V2Plot :=
  Plot[V2[t], {t, 0, 100 gyr},
   Ticks -> {{{6.31152 10^17, "20"}, {1.2623 10^18,
```

```
    "40"}, {1.89346 10^18, "60"}, {2.52461 10^18,
    "80"}, {3.15576 10^18, "100"}}, Automatic},
  PlotStyle -> {Thick, Red}];

In[225]:= Show[V1Plot,V2Plot]
Out[225]=
```

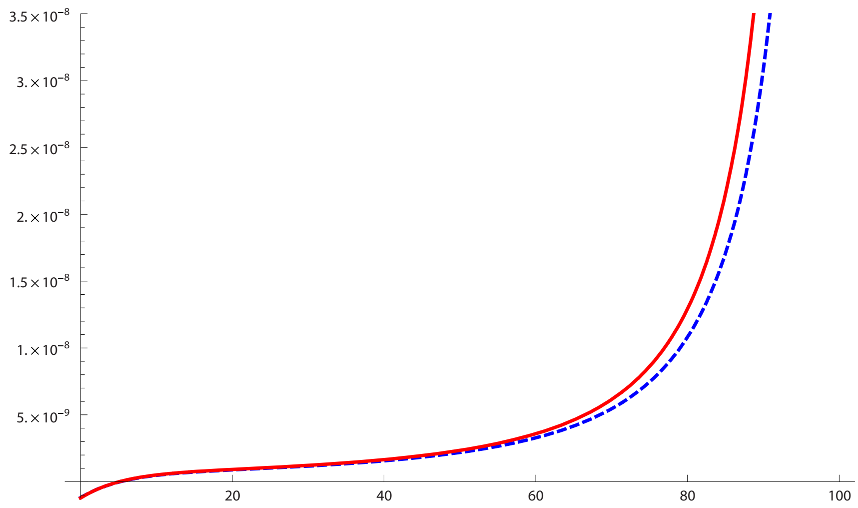


```
In[226]:= (* ========================================================== *)
(* Phantom scalar field solution (approximation) *)
Phi1[t_]:= Integrate[Sqrt[-((2 mp^2 c)/hbar *(q1/(trip1-t)^2))],t];
Phi2[t_]:= Integrate[Sqrt[-((2 mp^2 c)/hbar *(q2/(trip2-t)^2))],t];
Phi1[t]
Phi2[t]

Out[228]= -2.64197*10^13 Sqrt[1/(3.29818*10^18-1. t)^2]
(3.29818*10^18-1. t) Log[3.29818*10^18-1. t]

Out[229]= -2.63208*10^13 Sqrt[1/(3.22681*10^18-1. t)^2]
(3.22681*10^18-1. t) Log[3.22681*10^18-1. t]
```

```
(* ---------------------------------------------------------------- *)
(* It has some problem for t = 0, we must define new "phi"
(lowercase p) *)

phi1[t_]:= -2.641971739656076`*^13
*Sqrt[1/(3.2981831931995136`*^18-1.` t)^2]
*(3.2981831931995136`*^18-1.` t) Log[3.2981831931995136`*^18-1.` t];

phi2[t_]:= -2.6320782249292344`*^13
*Sqrt[1/(3.226806228094449`*^18-1.` t)^2]
*(3.226806228094449`*^18-1.` t) Log[3.226806228094449`*^18-1.` t];

(* ================================================================ *)
In[232]:= (* ===================== V(Phi) ===================== *)
(* Using "v" lowercase for v(\[Phi]) and "V" uppercase for V(t)
--- Indeed they are similar phantom potential *)

v1[Phi_]:= ((mp^2 c)/hbar)((3 q1^2 + q1)/Exp[(-2 Phi/alpha1)])
- d1 c^2 (trip1-tzero1)^(3 q1)/(2 Exp[((-3 q1) Phi/alpha1)]);

v2[Phi_]:= ((mp^2 c)/hbar)((3 q2^2 + q2)/Exp[(-2 Phi/alpha2)])
- d2 c^2 (trip2-tzero2)^(3 q2)/(2 Exp[((-3 q2) Phi/alpha2)]);

v1[\[Phi]]
v2[\[Phi]]
Out[234]= -2.516125664325231*10^-371 Exp[(-7.39612*10^-13 Phi)]
+ 6.47059*10^27 Exp[(7.5701*10^-14 Phi)]

Out[235]= -1.993330768839323*10^-368 Exp[(-7.36843*10^-13 Phi)]
```

```
+ 6.37163*10^27 Exp[(7.59856*10^-14 Phi)]

In[236]:= (* ================== Plot v(\[Phi]) ===================== *)
(* Blue-dashed for WMAP7+BAO+H0 dataset,
Red-thick for WMAP7 dataset alone *)

v1Plot:= Plot[v1[Phi],{Phi,phi1[0], phi1[100 gyr]},
PlotRange->{V1[0],3.5 10^(-8)},PlotStyle->{Thick,Dashed,Blue}]

v2Plot:= Plot[v2[Phi],{Phi,phi2[0], phi2[100 gyr]},
PlotStyle->{Thick,Red}];

Show[v1Plot,v2Plot]
Out[238]=
```

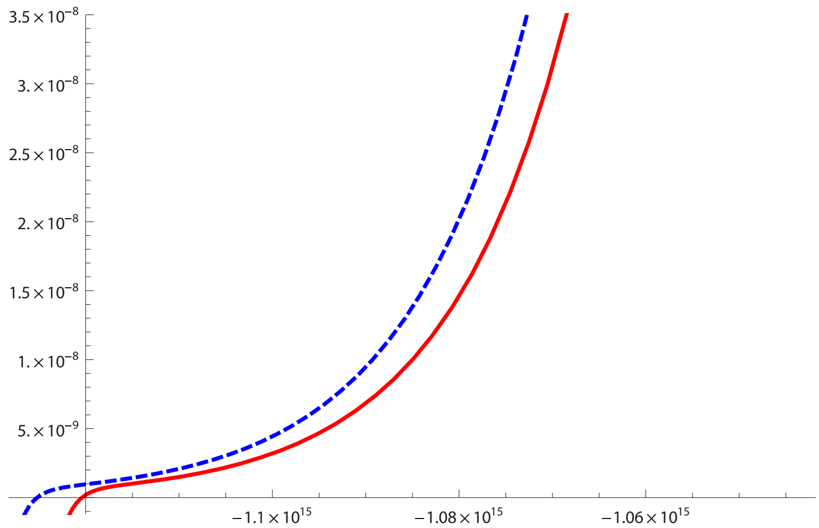


```
(* ================================================================ *)

In[239]:= (* energy density and pressure in the function of z *)
rhoz1[z_]:= (mp^2 c)/hbar *(3 q1^2 (1+z)^(2/q1))/(trip1-tzero1)^2
```

```
- d1 c^2(1+z)^3 ;
rhoz2[z_]:= (mp^2 c)/hbar *(3 q2^2 (1+z)^(2/q2))/(trip2-tzero2)^2
- d2 c^2(1+z)^3 ;
pz1[z_]:= -((mp^2 c)/hbar) *((3 q1^2-3q1)/(trip1-tzero1)^2)(1+z)^(2/q1)
-(d1 c^2(1+z)^3 )/2;
pz2[z_]:= -((mp^2 c)/hbar) *((3 q2^2-3q2)/(trip2-tzero2)^2)(1+z)^(2/q2)
-(d2 c^2(1+z)^3 )/2;

(* ================ w(z) ================== *)
wz1[z_]:=pz1[z]/rhoz1[z];
wz2[z_]:=pz2[z]/rhoz2[z];
(* ----------------------------------------- *)
In[245]:= wz1[z]
wz2[z]

Out[245]= (-(9.59505*10^-10/(1+z)^0.307057)
-1.13333*10^-10 (1+z)^3)/(8.318*10^-10/(1+z)^0.307057
-2.26666*10^-10 (1+z)^3)

Out[246]= (-(9.93584*10^-10/(1+z)^0.30937)
-1.12508*10^-10 (1+z)^3)/(8.60481*10^-10/(1+z)^0.30937
-2.25016*10^-10 (1+z)^3)

In[247]:= (* =============== At the Big Rip time ============== *)
Limit[wz1[z],{z->-1}]
Limit[wz2[z],{z->-1}]

Out[247]= {-1.15353}
Out[248]= {-1.15468}
```

```
(* ========================= End code ========================= *)
```

C.5 Code for estimation of error bars

```
In[1]:= (* Fundamental constants *)
c = 2.99792458*10^8;
g = 6.674*10^-11;
hbar = 1.055*10^-34;
(* ============================ *)

(* Reduced Planck mass *)
mp = Sqrt[(hbar*c)/(8Pi*g)];
(* ============================ *)

(* changing unit *)
gyr = 3.15576 10^16;
hunit = 10^(-19)/3.086;

(* ============================================================= *)
(* Observational parameter *)
(* --------- 1 for WMAP7+BAO+H0, 2 for WMAP7 alone ------------- *)
hzero1=70.2 hunit;           (* Hubble parameter *)
delhzero1Up = 1.3 hunit;     (* Error of H (upper and lower) *)
delhzero1Lo = 1.4 hunit;
hzero2=71.4 hunit;
delhzero2 = 2.5 hunit;
omegab1 = 0.0455 ;             (* baryonic density parameter*)
delOmgb1 = 0.0016 ;          (* Error of \Omaga_b *)
```

```
omegab2 = 0.0445;

delOmgb2 = 0.0028 ;

omegac1 = 0.227;              (* cold dark mater density parameter*)

delOmgc1 = 0.014  ;           (* Error of \Omaga_{CDM} *)

omegac2 = 0.217;

delOmgc2 = 0.026 ;

omegadust1:= omegab1+omegac1;(* cold dark mater density parameter*)

delOmgdust1:= Sqrt[(delOmgb1)^2+(delOmgc1)^2];(* Error of \Omg_m *)

omegadust2:=omegab2+omegac2;

delOmgdust2:= Sqrt[(delOmgb2)^2+(delOmgc2)^2];

tzero1:=13.78 gyr;            (* the present time *)

deltzero1 = 0.11 gyr;         (* Error of t_0 *)

tzero2:=13.71 gyr;

deltzero2 = 0.13 gyr;

(* ============================================================= *)


rhoc1 = (3 hzero1^2)/(8 Pi g);      (* Critical density *)

rhoc2 = (3 hzero2^2)/(8 Pi g);

rhom1 =  omegadust1 rhoc1;        (* Matter density *)

rhom2 =  omegadust2 rhoc2;


w = -1.12;                        (* Equation-of-state parameter *)


(* ========================================================*)

(* The Big Rip time *)

trip1 = tzero1-(2/3 ) 1/(1+w)*hzero1^-1*(1-omegadust1)^(-1/2);

trip2 = tzero2-(2/3 ) 1/(1+w)*hzero2^-1*(1-omegadust2)^(-1/2);

tripgyrunit1 = trip1/gyr;

tripgyrunit2 = trip2/gyr;
```

```
q1 = -hzero1 (trip1-tzero1) ;      (* Power-law exponent *)

q2 = -hzero2 (trip2-tzero2) ;


(* ============================================================== *)

In[39]:= (* Calculate error bar of trip *)

(* Changing variables, trip => ts[t0,H0,Omgm]

where ts->tzero, H0->hzero and Omgm->Omega_m0 *)


ts1[t01_,H01_,Omgm1_]:=t01-(2/3 ) 1/(1+w)*H01^-1*(1-Omgm1)^(-1/2);


Dt01:= Derivative[1,0,0][ts1][tzero1,hzero1,omegadust1];

DH01:= Derivative[0,1,0][ts1][tzero1,hzero1,omegadust1];

DOmgm1:= Derivative[0,0,1][ts1][tzero1,hzero1,omegadust1];


ts2[t02_,H02_,Omgm2_]:=t02-(2/3 ) 1/(1+w)*H02^-1*(1-Omgm2)^(-1/2);


Dt02:= Derivative[1,0,0][ts2][tzero2,hzero2,omegadust2];

DH02:= Derivative[0,1,0][ts2][tzero2,hzero2,omegadust2];

DOmgm2:= Derivative[0,0,1][ts2][tzero2,hzero2,omegadust2];


In[47]:= (* -------------------------------------- *)

(* Upper error bar of trip1 *)

deltrip1Up:= Sqrt[(Dt01 deltzero1)^2+(DH01 delhzero1Up)^2

+(DOmgm1 delOmgdust1)^2];


(* Lower error bar of trip1 *)

deltrip1Lo:= Sqrt[(Dt01 deltzero1)^2+(DH01 delhzero1Lo)^2

+(DOmgm1 delOmgdust1)^2];
```

```
deltrip1Up
deltrip1Up/gyr
deltrip1Lo
deltrip1Lo/gyr

Out[49]= 5.99383*10^16
Out[50]= 1.89933
Out[51]= 6.35751*10^16
Out[52]= 2.01457

In[53]:= (* -------------------------------------- *)
(* error bar of trip2 *)
deltrip2 := Sqrt[(Dt02 deltzero2)^2+(DH02 delhzero2)^2
+(DOmgm2 delOmgdust2)^2];

deltrip2
deltrip2/gyr

Out[54]= 1.09708*10^17
Out[55]= 3.47642

In[56]:= (* ================================================== *)
(* Calculate error bar of rhoc *)
(* -------------- rhoc1 -------------- *)

rhocrit1[H01_]:= (3 H01^2)/(8 Pi g);
Drhoc1:= rhocrit1'[hzero1];
delrhoc1Up:= Sqrt[(Drhoc1 delhzero1Up)^2];
delrhoc1Lo:= Sqrt[(Drhoc1 delhzero1Lo)^2];
```

```
delrhoc1Up
delrhoc1Lo

Out[60]= 3.42779*10^-28
Out[61]= 3.69146*10^-28

In[62]:= (* --------------- rhoc2 -------------- *)
rhocrit2[H02_]:= (3 H02^2)/(8 Pi g);
Drhoc2:= rhocrit2'[hzero2];
delrhoc2:= Sqrt[(Drhoc2 delhzero2)^2];

delrhoc2

Out[65]= 6.70458*10^-28

In[66]:= (* ==================================================== *)
(* Calculate error bar of rhom *)
(* -------------- rhom1 -------------- *)
delrhom1Up:= Sqrt[(rhoc1 delOmgdust1)^2+(omegadust1 delrhoc1Up)^2];
delrhom1Lo:= Sqrt[(rhoc1 delOmgdust1)^2+(omegadust1 delrhoc1Lo)^2];

delrhom1Up
delrhom1Lo

Out[68]= 1.60414*10^-28
Out[69]= 1.64701*10^-28

In[70]:=
```

```
delrhom2:=Sqrt[(rhoc2 delOmgdust2)^2+(omegadust2 delrhoc2)^2];

delrhom2

Out[71]= 3.05651*10^-28

In[72]:= (* ==================================================== *)
(* Calculate error bar of power-law exponent (q->beta )*)
(* -------------- q1 -------------- *)
delq1Up:= Sqrt[((tzero1-trip1)delhzero1Up)^2
+(-hzero1 deltrip1Up)^2+(hzero1 deltzero1)^2];

delq1Lo:= Sqrt[((tzero1-trip1)delhzero1Lo)^2
+(-hzero1 deltrip1Lo)^2+(hzero1 deltzero1)^2];

delq1Up
delq1Lo

Out[74]= 0.182214
Out[75]= 0.194553

In[76]:= (* -------------- q2 -------------- *)
delq2:=Sqrt[((tzero2-trip2)delhzero2)^2+(-hzero2 deltrip2)^2
+(hzero2 deltzero2)^2];
delq2
Out[77]= 0.340229
```

BIOGRAPHY

BIOGRAPHY

Name-Surname	Chakkrit Kaeonikhom
Date of Birth	November 26, 1983
Place of Birth	Nakhon Sawan, Thailand
Address	23 Moo 2 Tambon Nongbua, Nongbua District, Nakhon Sawan Province, Thailand 60110

Work Experiences

2009-2010	Teaching assistant in Introductory Physics Laboratory, Department of Physics, Naresuan University, Phitsanulok, Thailand
2007-2009	Teacher in Physics and General Science Naresuan University Secondary Demostration School, Phitsanulok, Thailand
2006-2007	Teacher in Physics and General Science Niyomsil Anusorn School, Phetchaboon Thailand

Education Background

2006	B.S. (Physics) Naresuan University Phitsanulok, Thailand

Publications

[1] Kaeonikhom, C., Gumjudpai, B. and Saridakis, E. N. (2011). Observational constraints on phantom power-law cosmology. **Phys. Lett. B**, 695(1-4), 45-54. [arXiv:1008.2182 [astro-ph.CO]].

[2] Kaeonikhom, C. (2011). Late-Time equation of state of phantom power-law cosmology. **Proceedings of 6$^{\text{th}}$ Siam Physics Congress**, (March), 31-34.